

# Robust Visual Question Answering: Datasets, Methods, and Future Challenges

Jie Ma, *Member, IEEE*, Pinghui Wang, *Senior Member, IEEE*, Dechen Kong<sup>†</sup>, Zewei Wang<sup>†</sup>, Jun Liu, *Senior Member, IEEE*, Hongbin Pei, and Junzhou Zhao

**Abstract**—Visual question answering requires a system to provide an accurate natural language answer given an image and a natural language question. However, it is widely recognized that previous generic VQA methods often exhibit a tendency to memorize biases present in the training data rather than learning proper behaviors, such as grounding images before predicting answers. Therefore, these methods usually achieve high in-distribution but poor out-of-distribution performance. In recent years, various datasets and debiasing methods have been proposed to evaluate and enhance the VQA robustness, respectively. This paper provides the first comprehensive survey focused on this emerging fashion. Specifically, we first provide an overview of the development process of datasets from in-distribution and out-of-distribution perspectives. Then, we examine the evaluation metrics employed by these datasets. Thirdly, we propose a typology that presents the development process, similarities and differences, robustness comparison, and technical features of existing debiasing methods. Furthermore, we analyze and discuss the robustness of representative vision-and-language pre-training models on VQA. Finally, through a thorough review of the available literature and experimental analysis, we discuss the key areas for future research from various viewpoints.

**Index Terms**—Visual question answering, bias learning, debiasing, multi-modality learning, vision-and-language pre-training.

## 1 INTRODUCTION

VISUAL Question Answering (VQA) aims to build intelligent machines that are able to provide a natural language answer accurately given an image and a natural language question about the image [1]. The goal of VQA, which bridges computer vision and natural language processing, is to teach machines to see and read simultaneously like humans. This task exhibits a multitude of applications, encompassing areas such as providing blind and visually-impaired individuals with information about the surrounding world, facilitating image retrieval in the absence of metadata [2], empowering intelligent virtual assistants [3], enabling visual recommendation systems [4], and contributing to autonomous driving [5]. For instance, we can use the VQA approach to query “Is there a panda in the image?” across all candidate images to identify those that contain pandas.

In the last few years, VQA has garnered significant attention in the research community [6], [7], [8], [9], [10], [11], which can be attributed to two key developments. First, a number of datasets, such as VQA v1 [1], VQA v2 [12] for fine-grained detection and recognition, FVQA [13], OK-VQA [14] for reasoning based on external knowledge, and GQA for compositional reasoning [15], have

been built to evaluate the ability of methods from different views. Second, a variety of VQA methods have been proposed, which can be classified into three groups [2]: joint embedding, attention mechanism, and external knowledge. Joint embedding-based methods [1], [16], [17], in particular, project image and question representations into a common space to predict answers. These methods typically learn coarse-grained multi-modal representations, which may bring noisy or irrelevant information into the prediction stage. To address this issue, attention mechanism-based methods [18], [19], [20], [21] usually fuse the representations of questions and images based on the learned importance of objects and words. In the real-world scenario, VQA often requires machines to understand not only image contents but also external prior information that ranges from common sense to encyclopedic knowledge. For instance, considering the question “How many fungal plants are there in the picture?”, the machine should comprehend the word “fungal” and know which plant belongs to this category. To this end, external knowledge-based methods [22], [23], [24] link the knowledge extracted from large-scale knowledge bases such as DBpedia [25], Freebase [26], and YAGO [27], into multimodality learning [28].

However, in parallel with the above works, several studies [29], [30], [31], [32], [33] found that the aforementioned generic methods tend to memorize statistical regularities or bias in the training data rather than ground images to predict answers. For example, in the middle bar chart of the fourth column of Fig. 1, we can see that “tennis” is the most frequent answer. These methods answer the questions of the second column mainly by exploiting the connections between critical words “what”, and “sports” of the questions and “tennis”. This will cause these methods to perform well in the In-Distribution (ID) test scenario that has similar

- <sup>†</sup> denotes the authors contribute equally to the work.
- Jie Ma, Pinghui Wang, Hongbin Pei, and Junzhou Zhao are with the Ministry of Education of Key Laboratory for Intelligent Networks and Network Security, School of Cyber Science and Engineering, Xi’an Jiaotong University, Xi’an, Shaanxi 710049, China.
- Dechen Kong and Zewei Wang are with the Ministry of Education of Key Laboratory for Intelligent Networks and Network Security, School of Automation Science and Engineering, Xi’an Jiaotong University, Xi’an, Shaanxi 710049, China.
- Jun Liu is with the Shannxi Provincial Key Laboratory of Big Data Knowledge Engineering, School of Computer Science and Technology, Xi’an Jiaotong University, Xi’an, Shaanxi 710049, China.

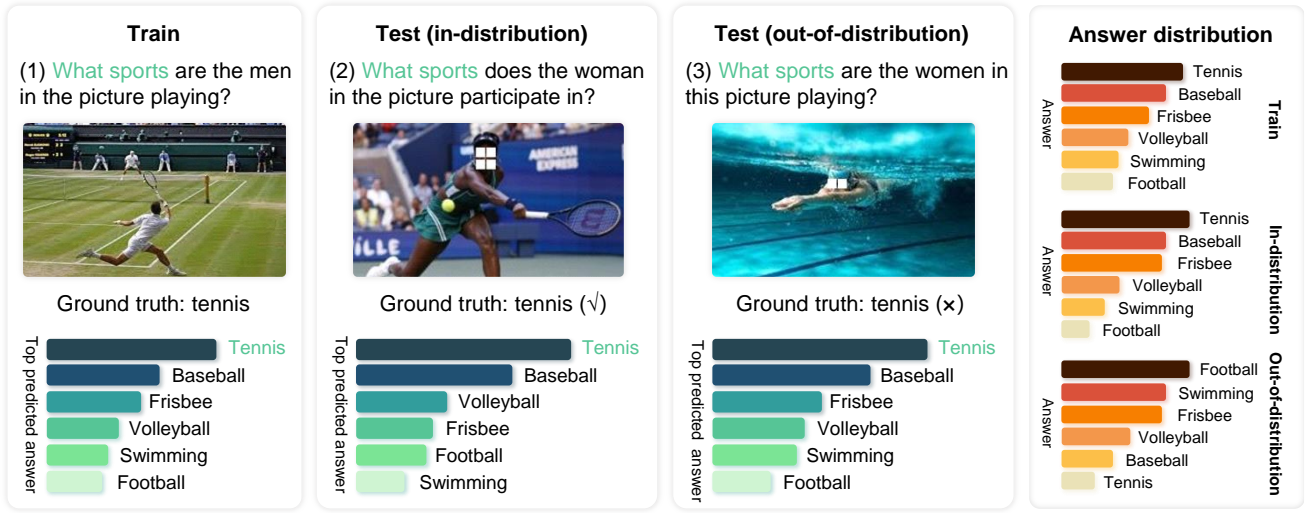


Fig. 1. Illustration of generic VQA methods in the in-distribution and out-of-distribution test scenarios. They predict answers by learning strong language bias, such as the connections between critical words “what”, and “sports” in questions and the most frequent answer “tennis”, rather than grounding images, which results in their high In-Distribution (ID) but poor Out-Of-Distribution (OOD) test performance. The ID situation refers to scenarios where the distribution is similar to that of the corresponding training split. The OOD scenario, on the other hand, applies to cases where the distribution differs or even opposes that of the training split.

answer distributions with the training split, such as the distribution in the middle bar chart of the fourth column, but poorly in the Out-Of-Distribution (OOD) test situation that has different or even reversed answer distributions, such as the distribution in the bottom bar chart. In order to address this issue, a significant body of literature on VQA has emerged in recent years, with a particular focus on eliminating bias [29], [34], [35] and evaluating robustness [29], [36], [37].

The purpose of this paper is to provide a comprehensive and systematic overview of the methods, datasets, and future challenges in the area of robust VQA. To the best of our knowledge, this paper is the first survey on the topic. In Section 2, we establish preliminary concepts for generic and robust VQA. Section 3 discusses the datasets from various perspectives including constructions, image sources, amounts of images and questions, and focuses. They are classified into two categories based on the ID and OOD settings. Section 4 reviews the evaluation metrics employed in the mentioned datasets including single and composite metrics. In Section 5, we undertake a critical analysis of debiasing methods, categorizing them into four classes: ensemble learning, data augmentation, self-supervised contrastive learning, and answer re-ranking. Section 6 reviews the development of representative vision-and-language pre-training methods and divides them into four classes based on the relative computational size of text encoders, image encoders, and modality interaction modules. We also discuss the robustness of these methods on the most commonly used VQA v2 [12] (ID) and VQA-CP (OOD) [29] datasets. Furthermore, in Section 7, we conduct in-depth discussions of future challenges from the perspective of improvements of annotation qualities, ongoing developments in dataset creation, evaluation metric advancements, method robustness, and robustness assessments, drawing on our experimental results and literature overview. Finally, we present our concluding remarks in Section 8.

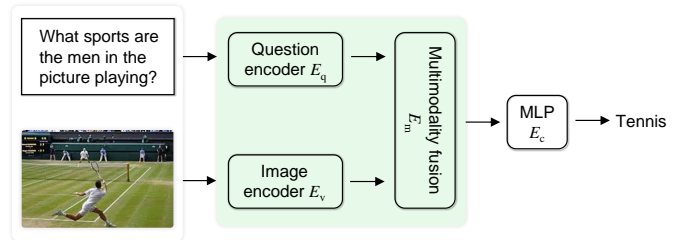


Fig. 2. Generic paradigm for VQA. This paradigm regards the image region (patch) and the question word as different types of tokens, while the other paradigm considers them to be the same kinds of tokens. Specifically, the latter always employs Transformer to replace  $E_q$ ,  $E_v$  and  $E_m$ .

## 2 PRELIMINARIES

In this section, we first describe the task formulation of VQA. Then, we briefly introduce the paradigm of current VQA methods. Finally, we define robust VQA methods from the perspective of debiasing.

**Task Formulation.** Given a dataset  $\mathcal{D}$  consisting of  $n$  triplets  $\{(v_i, q_i, a_i)\}_{i=1}^n$  with an image  $v_i \in \mathcal{V}$ , a question  $q_i \in \mathcal{Q}$ , and an answer  $a_i \in \mathcal{A}$ , VQA requires machines to optimize the parameters  $\theta$  and predict answers  $\hat{a}_i$  accurately:

$$\hat{a}_i = \arg \max_{a_i \in \mathcal{A}} p(a_i | v_i, q_i; \theta). \quad (1)$$

**Generic Paradigm.** Current non-debiasing (generic) methods [16], [19], [20], [38], [39], [40]  $f$  typically leverage an image encoder  $E_v : \mathcal{V} \rightarrow \mathbb{R}^{n_v \times d_v}$  to learn  $n_v$  region-level (patch-level) representations with  $d_v$  dimensions, a question encoder  $E_q : \mathcal{Q} \rightarrow \mathbb{R}^{n_q \times d_q}$  to output  $n_q$  word-level vectors with  $d_q$  dimensions, a multi-modality encoder  $E_m : \mathbb{R}^{n_q \times d_q} \times \mathbb{R}^{n_v \times d_v} \rightarrow \mathbb{R}^{d_m}$  to learn fusion representations with  $d_m$  dimensions, and a classifier  $E_c : \mathbb{R}^{d_m} \rightarrow \mathbb{R}^{|\mathcal{A}|}$  to obtain predictions over the answer space  $\mathcal{A}$ . The paradigm can be denoted as follows and shown in Fig. 2:

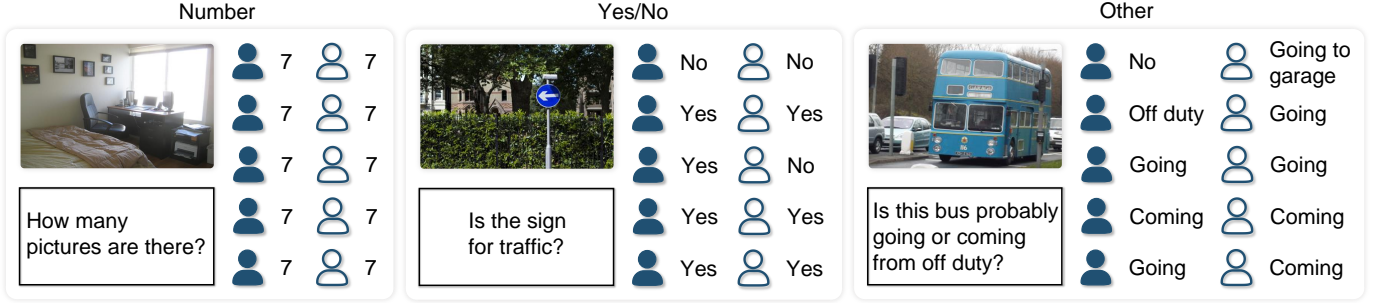


Fig. 3. VQA v1 example. Each question in this dataset is annotated by ten humans. Therefore, a question may exist multiple different ground-truth answers. The dataset is classified into three categories according to answer types: “Number”, “Yes/No”, and “Other”.

$$\hat{a}_i = f(v_i, q_i; \theta) = E_c(E_m(E_v(v_i), E_q(q_i))). \quad (2)$$

Furthermore, the success [41], [42], [43], [44], [45], [46] of Transformer in natural language processing has given rise to a new paradigm for VQA. Multiple studies [47], [48], [49] regard the image region (patch) and the question word as the same type of tokens and apply Transformer to learn multimodal representations. In other words, they leverage Transformer to replace  $E_q$ ,  $E_v$  and  $E_m$ . This paradigm can be denoted as follows:

$$\hat{a}_i = f(v_i, q_i; \theta) = E_c(\text{Transformer}(v_i || q_i)), \quad (3)$$

where  $v_i$  is the representation of regions or patches,  $q_i$  denotes the embeddings of words, and  $||$  represents the concatenation. This paradigm is always employed in large pre-trained vision-language models, which we will discuss separately in Section 6. Here, our primary focus will be on small models.

**Robust VQA.** Recent studies [29], [30], [34], [35] found that the generic methods are apt to exploit the training bias excessively rather than learn proper behaviors. For example, they may learn the spurious connections between critical words of questions and answers, such as “what”, “sports” and “tennis”. Therefore, the generic methods predict answers mainly relying on one of  $E_v(v_i)$  and  $E_q(q_i)$ . This can be formulated as follows:

$$\hat{a}_i = f_1(v_i, q_i; \theta_1) = E_c(E_q(q_i)), \quad (4)$$

$$\hat{a}_i = f_v(v_i, q_i; \theta_v) = E_c(E_v(v_i)), \quad (5)$$

where  $f_1$  refers to the language bias learning, and  $f_v$  represents the vision bias learning. According to the investigation in [29], [37], it has been found that language bias learning is more prevalent than vision bias learning.

Obviously, the mentioned bias learning will cause the generic methods to obtain high ID but poor OOD performance. In other words, the methods are incapable of dealing with various changing real-world situations. In comparison, on the basis of generic methods, debiasing methods aim at mitigating bias learning to achieve robust VQA performance in both scenarios. Formally, the debiasing method primarily focuses on acquiring a strategy to eliminate the impact of  $f_1$  or  $f_v$  on the  $f$  described in Equation (2) and (3).

### 3 DATASETS

A substantial volume of VQA datasets has been constructed encompassing diverse perspectives. This section presents a

comprehensive review of these datasets, categorizing them into two groups according to their ID and OOD settings.

#### 3.1 In-Distribution Setting

*ID settings typically represent that the test split’s distribution is similar to that of the corresponding training split.* A variety of ID datasets [1], [12], [15] have been developed from different angles and have made significant contributions to robust VQA research. These datasets can be particularly useful in evaluating the effectiveness of VQA methods, as they are specifically designed to assess various capabilities such as fine-grained detection and recognition, as well as common sense reasoning.

**VQA v1** [1]. This dataset was developed by asking ten human subjects the same question about a real image. As shown in the “other” question of Fig. 3, we can see that ten annotators produce five gold answers, including “No”, “Off duty”, “Going”, “Coming” and “Going to garage”. Therefore, the question in this dataset may exist several ground-truth answers.

VQA v1 is the first large-scale, open-ended, and free-form dataset to assess the ability of VQA methods such as fine-grained detection [50], [51], [52], recognition [53], [54], [55], and counting [56], [57]. The dataset consists of 614.2K questions accompanied by 204.7K images, where the questions are classified into three primary categories according to answer types: “Yes/No”, “Number”, and “Other”. Similar to the MS COCO dataset [58], VQA v1 is divided into six parts: training, validation, test-dev, test-standard, test-challenge, and test-reserve. The performance evaluation of test-dev, test-standard, and test-challenge can be obtained from the online server<sup>1</sup> after uploading the answer predictions of VQA methods. The default test data for the VQA competition is test-standard, while test-challenge is used to determine the competition winners. Test-reserve is utilized to prevent possible overfitting, and the results of this split are not publicly available. This competition has significantly stimulated the advancement of the VQA community.

However, Goyal *et al.* [12] found that VQA v1 contains strong language priors or bias. For example, the most common answer “tennis” is the correct answer for 41% of the questions starting with “what sport is”. This may drive VQA methods to answer questions depending on the bias rather than grounding images.

1. <https://eval.ai/web/challenges/challenge-page/830/overview>



Fig. 4. Illustration of balancing answer distributions in VQA v2. This dataset incorporates a complementary image that pertains to the same question in VQA v1 but has a different answer.

**VQA v2** [12]. To alleviate the mentioned dilemma, this dataset was developed by collecting complementary images for almost every question in VQA v1. Specifically, there are two images that appear to be similar but have different answers to the question. As shown in Fig. 4, VQA v2 adds a complementary image for the question “What sport is being played?” to mitigate the bias in VQA v1, where “badminton” is the complemented answer. In this way, the volume of VQA v2 is almost twice that of VQA v1, containing 1.1M questions with 479K images.

Despite achieving substantial success [59], [60], [61], [62], [63], VQA v2 still faces several issues [64], [65], [66], [67]. Firstly, the similarity between the distributions of training and test splits still exists, although the language prior is significantly weaker. Secondly, the simplicity of the question in the aforementioned dataset exacerbates the limitation stemming from the models’ dependence on statistical biases. Lastly, the absence of annotations pertaining to question structures and contents poses difficulties in comprehending the factors that influence model behaviors.

**GQA** [15]. To address the mentioned issues, this dataset was developed by leveraging the content provided by the scene graphs in Visual Genome [68], such as object information, attributes and relations, and structures from extensive linguistic grammar. Therefore, the question is more complex compared with that in VQA v2. Unlike VQA v1 and v2, each question in this dataset only has one ground-truth answer. GQA contains 22M questions with 113K images, which is split into four parts: training (70%), validation (10%), test (10%), and challenge (10%). Analogous to VQA v2, the result on this challenge split is applied to determine the competition winners<sup>2</sup>.

As shown in Fig. 5, GQA provides a scene graph [69] for each image and a functional program for each question. The scene graph exhibits the relations between objects such as the “to the right of” relation between “man” and “lady”, while the program delineates a series of reasoning steps required to derive answers. In other words, this dataset combines detailed visual annotations with question-answer pairs accompanied by succinct explanatory statements. Based on this, VQA models can associate individual words from questions and answers with visual pointers, guiding more attention to pertinent regions within the image [70]. Consequently, this dataset fosters the advancement of more explainable models that necessitate diverse reasoning and

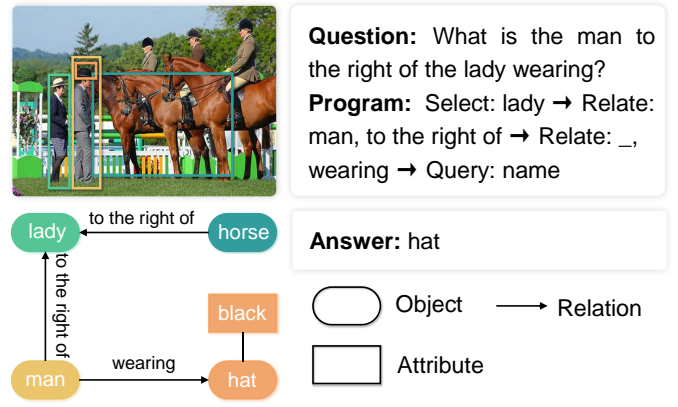


Fig. 5. GQA example. This dataset provides a scene graph for each image and a functional program for each question. The program enumerates a series of logical operations (reasoning steps) necessary to obtain the answer.

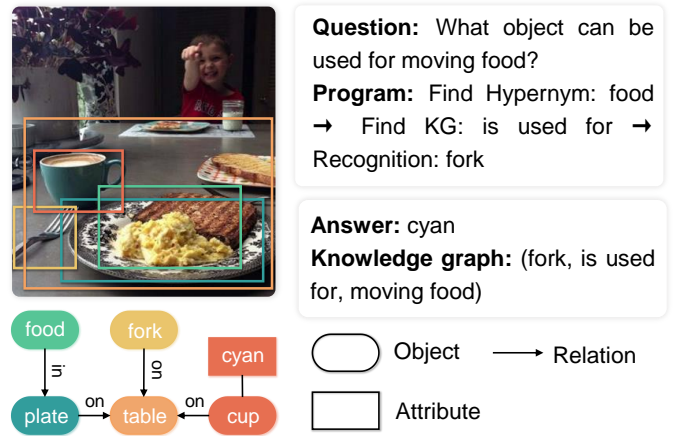


Fig. 6. CRIC example. This dataset provides additional object-level knowledge triples compared with GQA.

multi-step inference abilities, specifically by enhancing the comprehension of both visual and linguistic components in a refined manner. Nevertheless, GQA cannot evaluate the ability to query and fuse common sense due to the defect in dataset collections.

**CRIC** [71]. To solve the mentioned issue, this dataset<sup>3</sup> was developed by generating questions and corresponding annotations from the scene graph of a given image and a knowledge graph respectively. This dataset, which is split into three parts: training (70%), validation (10%), and test (20%), contains 494K questions with 96K images. To collect satisfactory knowledge items and generate compositional questions, the authors used a graph-to-graph format for representing the knowledge items, which is better at aligning entities in the knowledge graph to objects in the image and depicting the commonsense relations between objects. For instance, as shown in Fig. 6, it can be observed that this dataset not only includes identical components to GQA but also encompasses additional object-level knowledge triples such as the commonsense knowledge “(subject: fork, relation: is used for, object: moving food)”. Therefore, CRIC

2. <https://eval.ai/web/challenges/challenge-page/225/overview>

3. <https://cricvqa.github.io/>

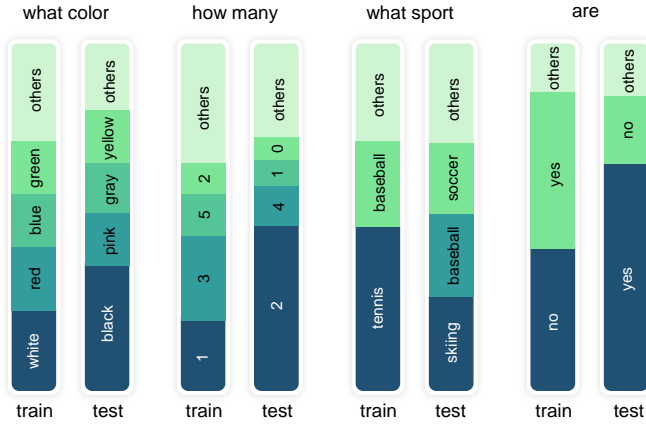


Fig. 7. Answer distributions under specific types of questions in VQA-CP v1 training and test splits.

requires machines to ground commonsense in the visual world and perform multi-hop reasoning on images and knowledge graphs.

Although the development of these datasets has promoted VQA research, some studies [29], [30], [34], [35] have revealed that existing methods tend to memorize or exploit the bias in the training data excessively rather than ground images first and then predict answers. To put it another way, the performance on the aforementioned datasets alone may not be a reliable indicator for VQA methods.

### 3.2 Out-of-Distribution Setting

To solve the mentioned issues, various OOD datasets have been developed successively, where *the distribution of the test split differs from or is even reversed to that of the training split*. These datasets aim to offer more challenging and intricate test scenarios from different perspectives, ranging from altering answer distributions to rephrasing questions. In this way, we are able to assess whether VQA methods can handle diverse real-world situations simultaneously or whether they are robust.

**VQA-CP v1 & VQA-CP v2** [29]. These two datasets were created by reorganizing VQA v1 and v2 according to the answer distribution, resulting in them sharing the same characteristics as VQA v1 and v2, such as multiple ground-truth answers for a single question. They are the first to explore the robustness evaluation of VQA methods, which motivates subsequent works [72], [73], [74], [75] to focus on VQA robustness. VQA-CP v1<sup>4</sup> contains 370K questions with 205K images, while VQA-CP v2 contains 658K questions with 219K images.

The distributions between the training and test splits of VQA-CP exhibit significant differences, and in some cases, they are even reversed. For instance, Fig. 7 shows that the most common answer to the question “what sport” in the training split of VQA-CP v1 is “tennis”, while in the test split, “skiing” emerges as the most prevalent answer. Therefore, these two datasets can be utilized to evaluate whether VQA methods predict answers through bias learning.

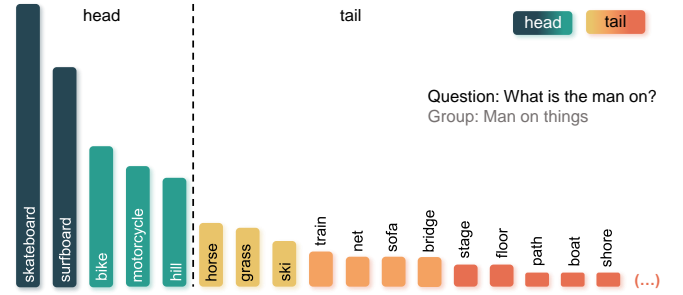


Fig. 8. Answer distributions or frequencies within the “Man on things” group. The “tail” group is utilized to evaluate the OOD performance, while the “head” group is employed to assess the ID performance.

However, these datasets are not without their limitations. Firstly, they consist of only two parts: a training set (67%) and a test set (33%), without including a validation set. This arrangement may lead to the tuning of hyper-parameters on the test split. Secondly, the introduction of artificially crafted distribution shifts may not accurately reflect real-world scenarios. Lastly, models developed based on these datasets tend to be tailored toward their specific configurations due to the manual crafting of these shifts, potentially resulting in reduced generalization capabilities. **GQA-OOD** [36]. To address the mentioned issues, this dataset<sup>5</sup> was developed by reorganizing GQA [15] in a fine-grained manner such that distribution shifts are introduced in both the validation and test splits, and are tailored to different question groups. Specifically, GQA-OOD divides questions into two groups: “head” and “tail”, according to the frequency of answers, instead of modifying the global distributions of the validation and test splits. As illustrated in Fig. 8, the answers to the “man on things” question group are classified into two groups based on a criterion of  $|a_i| \leq 1.2\mu(a)$ , where  $|a_i|$  denotes the number of samples within the class  $i$  such as “skateboard” and “surfboard”, and  $\mu(a)$  represents the average sample count for this group.

GQA-OOD contains 53K questions with 9.7K images, which is split into two parts: validation (95%) and testdev (5%). Each part has two subsets: “tail” and “head”. The “tail” group is used to evaluate the OOD performance, while the “head” group is employed to assess the ID performance. This dataset requires models to be trained on the original GQA training split. In this way, it compels models to minimize bias in their test results while simultaneously exposing the models to bias captured within the training data [36]. Therefore, this dataset promotes the intrinsic development of debiasing methods rather than relying solely on the purification of training data.

**VQA-Rephrasings** [76]. This dataset was developed by first considering the validation split of VQA v2.0 as the base set, then sampling from this set to form a subset, and finally collecting three human-provided rephrasing for each question in this subset. As illustrated in Fig. 9, the right questions are obtained by changing the expression of the left original question while retaining its original meaning. In this way, VQA-Rephrasings collects 162.0K questions with 40.5K images. This dataset enables the evaluation of VQA

4. <http://data.lip6.fr/cadene/murel/vqacp2.tar.gz>

5. <https://github.com/gqa-ood/GQA-OOD>

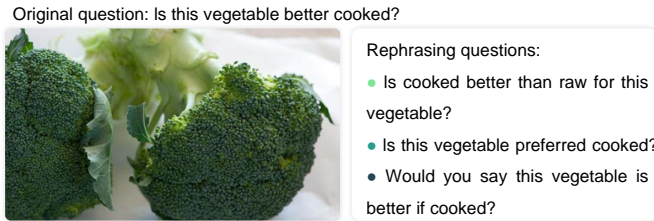


Fig. 9. VQA-Rephrasings example. The original question is selected from the validation split of VQA v2, while the rephrased question is collected from three humans under the condition of preserving the original meaning.

methods for robustness and consistency across alternative rephrasing of questions with the same meaning.

**VQACE** [77]. The previously mentioned datasets commonly overlook multimodal bias, instead prioritizing the assessment of language bias learning. Multimodal bias is such a phenomenon that the frequent co-occurrence of textual and visual elements within the training data predicts specific answers accurately. Similar to the language bias, multimodal bias often persists and transfers to the validation set, potentially impacting the generalizability of VQA models. In order to address this issue, Dancette *et al.* [77] proposed a method for identifying shortcuts that predicts the correct answer based on the appearance of words in the question and visual elements in the image. Then, they built VQA counter examples where the shortcut rules result in inaccurate answers as the evaluation protocol. As depicted in Fig. 10, VQA models may learn or memorize certain words such as “doing” and objects like “man”, “surfboard”, and “hand” to predict answers. Although this can result in accurate predictions for some examples (as seen in the left example), it can also lead to incorrect responses (as observed in the right example). There is also an easy subset in which the correct answers can be derived through at least one of the shortcuts. Statistics show that 90% of the bias in this dataset<sup>6</sup> is multimodal, indicating that previous successful debiasing methods [29], [30], [34], [35] in addressing the shift in language distributions such as the shift in VQA-CP and VQA-Rephrasings but may not be as effective in reducing natural shortcuts from VQA.

**VQA-VS** [37]. Like VQACE, this dataset<sup>7</sup> takes into account the natural shortcuts in VQA, such as language, vision, and multimodality bias. It goes a step further by introducing several concrete shortcuts for each bias, such as the question-type shortcut in language bias and the key-object-pair shortcut in vision bias. For instance, the multimodal bias of VQACE in Fig. 10 belongs to the shortcut of “composite of keyword and key object” in this dataset. These shortcuts may be used to assess OOD performance in a more refined manner. In addition, this dataset also includes a split to evaluate ID performance.

However, the datasets mentioned above have certain limitations [78]. Firstly, these datasets are mainly developed based on heuristic rules [29], [79], [80]. Furthermore, synthetic images or questions are often used in these datasets

Multimodal bias: { doing + man + surfboard + hand } → surfing

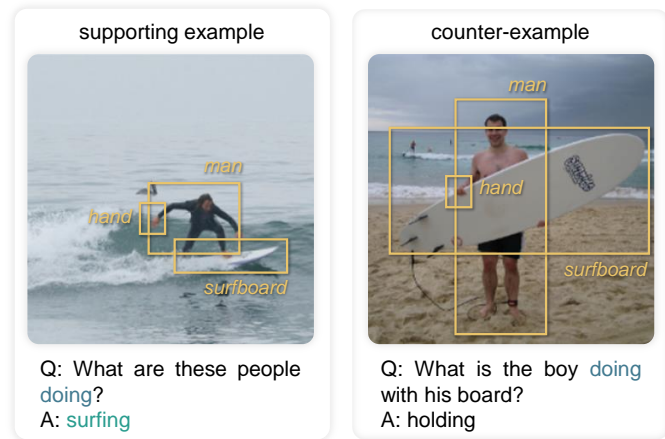


Fig. 10. Example of a multimodal shortcut in VQACE, with its supporting examples and counter examples. This shortcut is a combination of words “doing” and objects including “man”, “surfboard”, and “hand”. Generic VQA methods usually make accurate/wrong predictions when facing the left/right examples respectively.

[15], [79], [80], instead of being generated by humans. They may not represent real-world scenarios accurately.

**AVQA** [78]. To address the above issues, this dataset<sup>8</sup> was gathered iteratively using an adversarial “human-and-model-in-the-loop” procedure. The process of data collection can be viewed as a game played in  $n$  rounds between two parties: a human annotator and a well-trained model. AVQA consists of 243.0K questions accompanied by 37.9K images and is developed through three rounds. Specifically, the image-question pairs are gathered once VQA models that are trained on VQA v2 [12] and Visual Genome [68] cannot predict answers accurately. To avoid over-fitting, the VQA model is randomly chosen from LXMERT [81], UNITER-B [48], and UNITER-L [48]. To collect harder questions, the model is re-trained based on the data collected from previous rounds. Note that the question is written by humans rather than rule-based questions such as in GQA. Therefore, AVQA may be more challenging than previous datasets [12], [67], [68], [82], [83], [84].

**AdVQA** [87]. Similar to AVQA, this dataset<sup>9</sup> was also developed by the human-and-model-in-the-loop procedure [88]. In other words, both of them are developed from the perspective of adversarial robustness. This dataset contains 46.8K questions accompanied by 41.8K images. In comparison, the developing procedure for this dataset has an additional question validation phase, which manually determines whether the image is necessary and sufficient to answer the question.

In a nutshell, each dataset has a distinct focus and can be used to assess the ability of methods from a particular angle. More details of datasets, such as the source of images and the focus, are shown in Table 1.

6. <https://github.com/cdancette/detect-shortcuts>

7. <https://github.com/PhoebusSi/VQA-VS>

8. <https://adversarialvqa.org/>

9. <https://adversarialvqa.org/>

TABLE 1

Comparison of datasets and evaluation metrics. ID denotes in-distribution, and OOD represents out-of-distribution. A single graph denotes a scene graph of an image. Double graphs denote scene and knowledge graphs. CC [85] is the dataset of conceptual captions. Fakeddit [86] is a multimodal dataset for fake news detection. Natural shortcuts include language, vision, and multimodality bias.

Dataset	Development	Image Source	Images	Questions	Focus	ID	OOD	Metrics
VQA v1 [1]	asking human questions	COCO	204.7K	614.2K	vision	✓	✗	open-ended accuracy
VQA v2 [12]	complement on VQA v1	COCO	479K	1.1M	vision	✓	✗	open-ended accuracy
GQA [15]	generate questions from a single graph	Visual Genome	113K	22M	composition	✓	✗	composite metrics
CRIC [71]	generate questions from double graphs	Visual Genome	96K	494.3K	commonsense	✓	✗	composite metrics
VQA-CP v1 [29]	reorganization on VQA v1	COCO	205K	370K	language bias	✗	✓	open-ended accuracy
VQA-CP v2 [29]	reorganization on VQA v2	COCO	219K	658K	language bias	✗	✓	open-ended accuracy
GQA-OOD [36]	reorganization on GQA	Visual Genome	82.2K	996.8K	language bias	✓	✓	composite metrics
VQA-Rephrasings [76]	rephrasing on VQA v2	COCO	40.5K	162.0K	language bias	✗	✓	consensus score
VQA-CE [77]	reorganization on VQA v2	COCO	-	-	natural shortcuts	✗	✓	open-ended accuracy
VQA-VS [37]	reorganization on VQA v2	COCO	-	-	natural shortcuts	✓	✓	open-ended accuracy
AVQA [78]	human-and-model-in-the-loop	CC/Fakeddit/VCR	37.9K	243.0K	adversarial robustness	✗	✓	open-ended accuracy
AdvQA [87]	human-and-model-in-the-loop	COCO	41.8K	46.8K	adversarial robustness	✗	✓	open-ended accuracy

## 4 EVALUATIONS

The evaluation is usually associated with the annotation of datasets, which ranges from open-ended accuracy to composite metrics. Existing debiasing works [30], [89], [90], [91] typically employ a combination of ID and OOD datasets to assess robustness. As a result, a trade-off metric such as the harmonic mean is used to assess the performance of methods comprehensively. The evaluation metrics of the mentioned datasets in Section 3 are shown in Table 1.

**Open-Ended Accuracy.** Given an image and its related question, humans may provide various answers in real-world scenarios. For example, “off duty” and “coming” are provided for the question that is on the right of Fig. 3 by different individuals. To comprehensively evaluate VQA methods, the questions in VQA v1 [1] and v2 [12] are annotated by ten humans, resulting in the employment of open-ended accuracy. Various datasets, such as VQA-CP [29] and VQA-CE [77], also use this metric because their development is related to the mentioned two datasets. The open-ended accuracy is computed as follows:

$$\text{open-ended accuracy} = \min \left\{ \frac{n_a}{3}, 1 \right\}, \quad (6)$$

where  $n_a$  denotes the number of predicted answers that are identical to human-provided answers for questions.

**Composite Metrics.** Unlike the datasets mentioned above, GQA [15] only contains an answer for each question, making it possible to use the “standard accuracy” as evaluation metrics. In addition, this dataset introduces five new metrics to gain a better understanding of visual reasoning techniques and highlights the functions that coherent reasoning methods should have.

- “Consistency” assesses the consistency of predicted answers across different questions. For example, given a question-answer pair “(Is there a banana to the right of the white cup?, Yes)” and an image, we can infer the answers to questions such as “Is there a fruit to the right of the white cup?” and “Is the white cup to the left of the banana?”.
- “Validity” and “Plausibility” are used to evaluate whether the predicted answer is reasonable enough. The former checks whether a given answer is within the scope of the question, such as providing colors to a color-type question. The latter goes a step further,

determining whether the answer makes sense, for example, pandas do not have the ability to talk.

- “Distribution” assesses the overall match between the true answer distribution and the method’s predicted distribution using Chi-Square statistics [92]. This metric enables us to evaluate the ability of models to predict not only the most frequent answers but also the less common ones.
- “Grounding” evaluates how well the model concentrates on regions of the image that are crucial to the question.

As introduced in the above subsection, GQA-OOD is developed by re-splitting the validation and test splits of GQA into *head* and *tail* groups respectively. Therefore, we can also use these five metrics to evaluate VQA methods besides the “head” and “tail” accuracy.

In addition to these metrics, there also exist other composite metrics to evaluate VQA performance. Specifically, CRIC [71] requires methods not only to predict answers but also to provide intermediate grounding results to mitigate the impact of commonsense prior and enables us to fairly evaluate whether methods truly understand the image and commonsense. In other words, a VQA system should provide two outputs for each question including an answer and a chosen object from the image. As a result, a question is considered to be correctly answered when the two predictions are both correct.

**Consensus Score.** To measure the robustness of methods across various question rephrasing, VQA-Rephrasings [76] introduces a metric dubbed “consensus score” based on the premise that the answer to all rephrasing of the same question should be the same. For instance, a system should provide the same answer given the four questions in Fig. 9. This consensus score  $cs$  is defined as the ratio of the number of subsets where all the answers are correct and the total number of subsets with size  $k$ :

$$cs(k) = \sum_{\mathcal{Q}' \subset \mathcal{Q}, |\mathcal{Q}'|=k} \frac{s(\mathcal{Q}')}{n C_k}, \quad (7)$$

$$\text{with } s(\mathcal{Q}') = \begin{cases} 1 & \text{if } \forall q \in \mathcal{Q}' \quad \phi(q) > 0, \\ 0 & \text{otherwise.} \end{cases},$$

where  $n C_k$  denotes the number of subsets with size  $k$  sampled from a set with size  $n$ ,  $\mathcal{Q}'$  denotes a group of

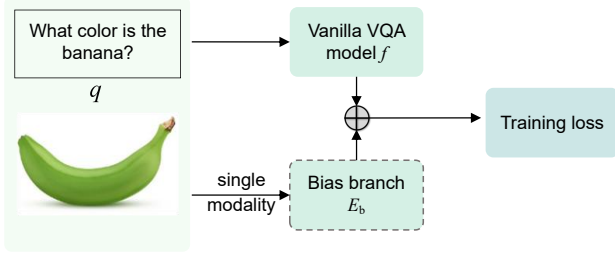


Fig. 11. Illustration of ensemble learning-based debiasing methods. The bias branch takes single modalities as inputs to capture bias learning in the training stage. In the test stage, the branch is removed, and answers are provided by the vanilla VQA model.  $\oplus$  denotes the combination operation such as a sigmoid function.

questions contained in  $\mathcal{Q}$ , and  $\phi(q)$  is a non-zero accuracy that is defined in [93].

## 5 DEBIASING METHODS

In recent years, based on generic methods such as UpDn [19], BAN [94], SMRL [20], and LXMERT [81], a variety of VQA debiasing methods [33], [95], [96] have been proposed to improve robustness. We divide these methods into four categories according to the debiasing technique: *ensemble learning*, *data augmentation*, *self-supervised contrastive learning*, and *answer re-ranking*. Table 2 presents their typology as well as their performance on both the VQA-CP v2 [29] test split and the VQA v2 [12] validation split.

### 5.1 Ensemble Learning

Ensemble learning-based methods are the first to investigate the robustness of VQA. They typically apply the combination  $\Phi$  of a bias branch  $E_b$  and a vanilla VQA method  $f$  defined in Equation (2) to predict answers  $\hat{a}_i$  comprehensively.  $E_b$  is used to capture the bias learning, while  $f$  is applied to perform normal question answering. This process can be denoted as follows:

$$\hat{a}_i = \Phi(E_b(E_v(v_i), E_q(q_i)), f(v_i, q_i)). \quad (8)$$

The illustration of the ensemble learning-based method is shown in Fig. 11. *In the training stage*, a single modality, such as questions alone, is fed into the bias branch, irrespective of images. In this way, the accurate prediction of the answer can be achieved to a great extent without relying on the visual information provided by the image modality. In other words, the bias or statistical correlations in the training data are captured. Then, the bias branch and the vanilla method are trained in an ensemble manner. For example, their predictions are combined by a sigmoid function [34]. Since the bias has been captured by the branch module, the vanilla method has no incentive to learn those superficial correlations. *In the test stage*, the vanilla method is used alone to provide unbiased predictions.

Specifically, RUBi [34], LMH [103], and AdvReg [100] leverage a question-only branch with a specific mechanism, such as a sigmoid function, a learned mix-in [97] strategy, and an adversarial regularization, respectively, to prevent the vanilla method from looking into only one modality. It is noteworthy that this branch is usually implemented by

a Recurrent Neural Network (RNN) followed by a multi-layer perceptron. GGE [122] decomposes the language bias into two categories, namely distribution bias and shortcut bias. To mitigate them, it employs a greedy gradient ensemble training strategy. The architecture of GGE is also a combination of the question-only branch and the vanilla VQA model  $f$ . Inspired by the causal effect, CF [120] revisits ensemble-based debiasing methods from a causal inference perspective, formulating the language bias as the direct causal effect of questions on answers, *i.e.*, the pure language effect. It mitigates the bias learning by subtracting the pure language effect from the total causal effect.

However, the above methods still suffer from the issue of achieving high OOD performance at the expense of ID performance. To address this problem, IntroD [30] introduces a training paradigm that first applies CF as a causal teacher to capture the bias in ID and OOD scenarios, then blends the inductive bias of both worlds fairly, and finally performs distillation for a robust student model. Inspired by the above works, CIKD [121] jointly investigates the causal effect [136], [137], knowledge distillation [138], [139], and ensemble learning to address the influence of bias. However, these methods can hardly benefit from language bias. Curriculum learning [140] enables models to be trained initially on the easier examples and gradually shift towards the harder ones. Motivated by this, LBCL [72] leverages a visually sensitive coefficient metric to measure the difficulty of each sample and applies an easy-to-hard training strategy to solve the bias learning. D-VQA [126] aims to mitigate the impact of negative bias in language and vision modalities by considering both feature-level and example-level perspectives. From the feature-level view, it leverages a question-only and image-only branch to capture the uni-modal bias respectively. From the example-level view, it builds negative examples to assist the model training.

### 5.2 Data Augmentation

Data augmentation-based methods typically generate additional augmented question-answer pairs  $(v_i, q_i, a_i')$  for each sample in the original dataset  $\mathcal{D}$  to balance the distribution of training data or mitigate the data bias. In particular, the question  $q_i$  is generated using word masking or replacement [61], [120], the image  $v_i$  is produced by object swapping and mixing [141], color conversion [142], and image flipping and resizing [143], and the answer  $a_i'$  is obtained by the devised answer-assigning mechanism. The answer prediction  $\hat{a}_i$  process is the same as the paradigm described in Equation (2):

$$\hat{a}_i = E_c(E_m(E_v(v_i), E_q(q_i))), \quad (9)$$

$$(v_i, q_i, a_i) \in \mathcal{D} \cup \{(v_i', q_i', a_i') | i \in [1, n]\}.$$

The methods usually perform data augmentation from two perspectives to achieve robust performance: 1) *synthetic-based*: generate new training samples by modifying regions or words of the original images or questions; 2) *pairing-based*: generate new samples by re-matching relevant questions for images. The examples generated by the mentioned techniques are shown in Fig. 12. The left is an original sample, while the right is the augmented sample based on the left sample. The synthetic method masks the “sheep” region in the image, resulting in the original question having a new



TABLE 2

The typology and performance of existing debiasing methods. HM denotes the harmonic mean of overall accuracy. ● represents the main category that a method belongs to, while ○ denotes the method that also uses the other debiasing technique. The result marked in bold is the best performance on the dataset. The result of the method with two references following is reported by the latter reference. LM denotes the Learned Mixin [97], while LMH denotes LM with an entropy penalty.

Method	Base	Year	Ensemble Learning	Data Augmentation	Self-Supervised Contrastive Learning	Answer Re-Ranking	VQA-CP v2 test	VQA v2 validation	HM
Template-based [98], [99]	UpDn	2017		●			39.75	63.83	48.99
GVQA [29]	SAN	2018				●	31.30	48.24	37.97
AdvReg [100], [101]	UpDn	2018	●				41.17	62.75	49.72
AttAlign [102]	UpDn	2019				●	39.37	63.24	48.53
RUBi [34]	UpDn	2019	●				47.11	61.16	53.22
HINT [102]	UpDn	2019				●	46.73	63.38	53.80
LMH [103]	UpDn	2019	●				52.87	55.99	54.39
SCR [101]	UpDn	2019				●	49.45	62.20	55.10
ASL [104]	UpDn	2019		●			46.00	-	-
DLR [105]	SAN	2020				●	34.83	49.27	40.81
CSS+CL [89]	UpDn	2020	○	○	●		40.49	-	-
CVL [106]	UpDn	2020		●			42.12	-	-
CVL [106]	Pythia	2020		●			-	68.77	-
GradSup [107]	UpDn	2020		●			46.80	-	-
RankVQA [108]	UpDn	2020				●	43.05	65.42	51.93
DLR [105]	UpDn	2020				●	48.87	57.96	53.03
SimpleReg [109]	UpDn	2020				●	48.90	62.60	54.91
MFE [110]	LMH	2020	○			●	58.21	53.15	55.57
VGQE [111]	SMRL	2020		●			50.11	63.18	55.89
RandImg [112]	UpDn	2020		●			55.37	57.24	56.29
CSS+CL [89]	LMH	2020	○	○	●		59.18	57.29	58.22
VILLA [113]	-	2020		●			49.10	74.69	59.25
CSS [90]	LMH	2020	○	●			58.95	59.91	59.43
MANGO [114]	-	2020		●			52.76	74.26	61.69
MUTANT [115]	UpDn	2020		●			61.72	62.56	62.14
X-GGM [95]	-	2021		●			-	-	-
MCE [116]	-	2021	●				-	-	-
LPF [73]	BAN	2021	○			●	50.76	-	-
LPF [73]	SMRL	2021	○			●	53.38	-	-
LBCL [72]	-	2021	●				60.74	-	-
AdVQA [117], [118]	-	2021	●				54.67	46.98	50.53
Unshuffling [119]	UpDn	2021		●			43.37	63.47	51.53
IntroD [30]	RUBi	2021	●				48.54	61.86	54.40
IntroD [30]	LMH	2021	●				51.31	62.05	56.17
LPF [73]	UpDn	2021	○			●	51.57	62.63	56.56
CF [120]	SMRL	2021	●				53.55	60.94	57.01
CIKD [121]	UpDn	2021	●				54.05	61.29	57.44
SimpleAug [99]	LMH	2021		●			53.70	62.63	57.82
SimpleAug [99]	UpDn	2021		●			52.65	64.34	57.91
GGE [122]	UpDn	2021	●				57.32	59.11	58.20
CF [120]	UpDn	2021	●				55.05	63.73	59.07
CCB [123]	HINT	2021	○			●	59.12	59.17	59.14
CCB [123]	UpDn	2021	○			●	57.99	60.73	59.32
LP-Focal [124]	UpDn	2021				●	58.45	62.45	60.38
SSL [125]	UpDn	2021		○	●		57.59	63.73	60.50
IntroD [30]	CSS	2021	●				60.17	62.57	61.35
D-VQA [126]	UpDn	2021	●		○		61.91	64.96	63.40
SAR [127]	LMH	2021	○			●	66.73	69.22	67.95
SimpleAug [99]	LXMERT	2021		●			62.24	<b>74.98</b>	68.02
SwapMix [35]	-	2022		●			-	-	-
Loss-Rescaling [128]	UpDn	2022				●	47.09	55.50	50.95
Loss-Rescaling [128]	LMH	2022				●	53.26	56.81	54.98
Loss-Rescaling [128]	CSS	2022				●	50.73	61.14	55.45
Loss-Rescaling [128]	LM	2022				●	53.17	59.45	56.13
Loss-Rescaling [128]	CSS+LMH	2022				●	56.55	55.96	56.25
ECD [129]	UpDn+LMH	2022	○	●			59.92	57.38	58.62
MMBS [130]	LMH	2022	○	○	●		56.44	61.87	59.03
KDDAug [131]	RUBi	2022		●			59.25	60.25	59.75
KDDAug [131]	LMH	2022		●			59.54	62.09	60.79
VQA-BC [91]	LMH	2022	○	○	●		60.81	61.74	61.27
AttReg [132]	LMH	2022	○	●			60.00	62.74	61.34
KDDAug [131]	UpDn	2022		●			60.24	62.86	61.52
KDDAug [131]	CSS	2022		●			61.14	62.17	61.65
Loss-Rescaling [128]	LXMERT	2022				●	66.40	69.76	<b>68.04</b>
RMLVQA [118]	UpDn	2023	○			●	60.41	59.99	60.20
GGD [133]	UpDn	2023	●				59.37	62.15	60.73
GenB [134]	LXMERT	2023	●				<b>71.16</b>	-	-
LSP [135]	UpDn	2023	○	○	●		61.95	65.26	63.56

answer “0”. Compared with this, the pairing method does not change the original image instead of retrieving related questions to it.

**Synthetic-based.** Kafle *et al.* [98] used existing semantic annotations in the dataset and RNN-based methods to produce new questions respectively. Agarwal *et al.* [79]

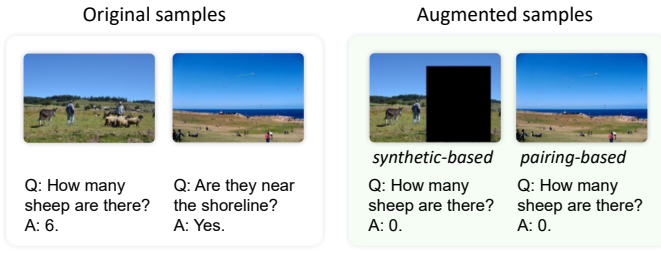


Fig. 12. Comparison between original samples and augmented samples. The synthetic-based technique generates new training samples by modifying regions or words of the original images or questions, while the pairing-based technique generates new samples by re-matching relevant questions for images.

leveraged a GAN-based model [144] to remove objects and then mitigated the bias by adversarial training. An ideal VQA model should possess two key characteristics [90]: (1) visual-explainable ability: the model should make accurate predictions by leveraging relevant visual regions. (2) question-sensitive ability: the model should be sensitive to different questions, *i.e.*, the model is expected to yield varying responses for different questions. To address this issue, CSS [90] and ECD [129] first synthesize counterfactual image-question pairs by masking critical objects in the original image and critical words in the original question and then assign ground-truth answers to those synthesized samples. This can drive the method to employ informative data to answer questions. In order to force the method to concentrate on the critical elements of inputs, MUTANT [115] performs mutating on the input images and questions to expose the model to perceptually similar yet semantically dissimilar samples.

**Pairing-based.** To make the synthesized samples more natural, SimpleAug [99] utilizes rich semantic annotations in the training data to pair images with other relevant questions, instead of generating them from scratch and employs a series of rules to ascertain the existence of ground-truth answers. However, the reasonable answers generated by the mentioned rules may limit the generalization. To address this issue, KDDAug [131] relaxes the requirements for reasonable image-question pairs and generates pseudo-answers for all composed pairs using a knowledge distillation-based answer assignment.

There also exist other alternatives to achieve the purpose of data augmentation. Specifically, DLR [105] decomposes the question representation into three distinct phrase representations: type, object, and concept, which are then integrated to predict answers. VGQE [111] learns question representations by leveraging both visual information extracted from the image and linguistic information derived from the question prior to multimodal fusion. CVL [106] uses a causal model with an additional variable to generate counterfactual samples, which compels the VQA model to utilize both input modalities instead of depending on statistical patterns that are specific to either one. The aforementioned methods [79], [90], [129], [131] augment data based on the internal (original) data. Compared with this, we can also expand data from the external source. For instance, inspired by meta-learning [145], [146], [147], ASL [104] retrieves the rel-

evant samples with image-question pairs from an external source, which is leveraged to learn adapting parameters for the VQA baseline, such as UpDn [19], thus acquiring better generalization ability.

### 5.3 Self-Supervised Contrastive Learning

Self-supervised contrastive learning [148], [149], [150] aims at learning an embedding space where similar sample pairs are positioned closely together while dissimilar ones are widely separated. Its use in robust VQA is still at the starting stage. The paradigm of contrastive learning-based debiasing methods is to first generate positive and negative samples that differ from the original samples using data-augmentation techniques introduced in the above subsection, then perform question answering by the vanilla VQA method  $f$  described in Equation (2), and finally be optimized jointly by the contrastive learning loss  $\mathcal{L}_C$  of multimodal representations and the VQA loss  $\mathcal{L}_V$ , as shown in Fig. 13. The joint loss  $\mathcal{L}$  can be formulated as follows:

$$\begin{aligned} \mathcal{L} &= \lambda_C \mathcal{L}_C + \lambda_V \mathcal{L}_V, \\ \mathcal{L}_C &= \mathbb{E}_{o,p,n \in \mathcal{D}^*} \left[ -\log \left( \frac{e^{s(o,p)}}{e^{s(o,p)} + e^{s(o,n)}} \right) \right], \\ \mathcal{L}_V &= -\frac{1}{|\mathcal{D}^*|} \sum_{i=1}^{|\mathcal{D}^*|} [a_i] \log \hat{a}_i, \end{aligned} \quad (10)$$

where  $\lambda_C$  and  $\lambda_V$  are used to balance contrastive learning and VQA,  $s(o,p)$  is the scoring function between the anchor  $o$  and the positive sample  $p$ ,  $s(o,n)$  is the scoring function between the anchor  $o$  and the negative sample  $n$ ,  $|\mathcal{D}^*|$  denotes the number of samples in the augmented dataset such as the dataset described in Equation (9), and  $[a_i]$  is the index of the answer  $a_i$ .

Specifically, CSS+CL [89] is the first to introduce self-supervised contrastive learning for VQA counterfactual samples, where CSS [90] is leveraged to generate factual and counterfactual samples or positive and negative samples. Nevertheless, it has been found that CSS+CL results in a decline in ID performance while only slightly improving OOD performance. To this end, MMBS [130] attributes the key point of solving language bias to the positive-sample design for excluding spurious correlations, which can boost the OOD performance significantly while retaining the ID performance. It exploits unbiased information through a positive sample construction strategy and employs an algorithm to discriminate between biased and unbiased samples so that they can be handled differently. These methods mitigate training bias from the forward chaining perspective which is similar to the paradigm described in Equation (2), but they rarely explore it from the backward chaining perspective. Motivated by this, Lao *et al.* [91] introduced a bidirectional chaining framework. In this framework, the forward chaining process resembles the procedure described in Equation (2). On the other hand, the backward chaining process aims to generate crucial visual features by leveraging the annotated answer as a guiding mechanism. Nonetheless, the negative sample generation techniques employed by the aforementioned methods may inadvertently introduce visual shortcut bias [77]. To tackle this problem,

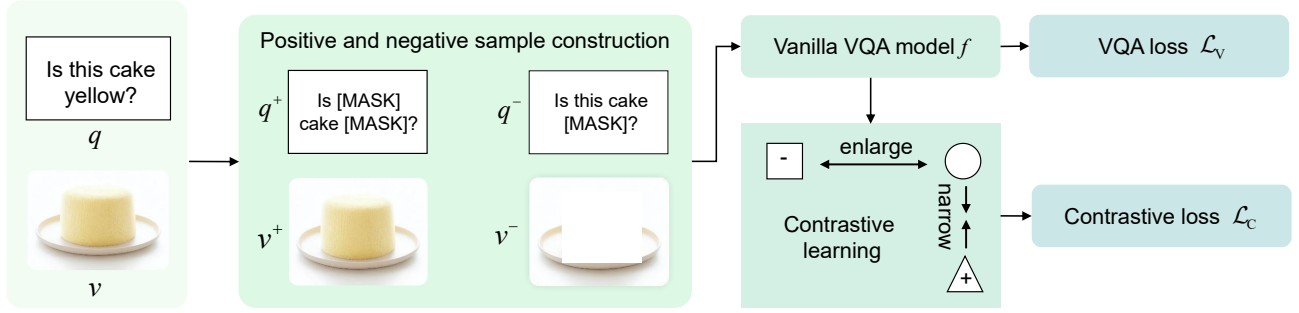


Fig. 13. Illustration of self-supervised contrastive learning-based debiasing methods. The contrastive learning loss  $\mathcal{L}_C$  is calculated by narrowing the distance between similar samples and enlarging the distance between dissimilar samples in the multi-modal joint embedding space. The model is trained by jointly optimizing VQA and contrastive losses.

LSP [135] introduces selective sampling rates and question-type-guided sampling, effectively eliminating the reliance of VQA models on visual shortcut bias. Furthermore, drawing inspiration from prompt learning [151], [152], [153], LSP introduces a question-type-guided prompt within the language context, thereby enhancing the significance of questions within the VQA model.

#### 5.4 Answer Re-Ranking

The answer re-ranking-based methods employ the re-ranking mechanism to re-sort the candidate answers provided by vanilla VQA baselines, which can guide the baseline to make better use of visual information. Specifically, their paradigm is to first predict answers using the vanilla method  $f$  described in Equation (2), and then re-rank answers leveraging the re-ranking module  $E_r$ , and finally guide  $f$  to provide accurate answers  $\hat{a}_i$  by back-propagating the gradient of re-ranking losses, as shown in Fig. 14. This process is formulated as follows:

$$\hat{a}_i = E_r(E_c(E_m(E_v(v_i), E_q(q_i))))). \quad (11)$$

Specifically, GVQA [29] decouples the recognition of visual objects in an image from the identification of plausible answer space for a given question. This is accomplished through the use of a question classifier, which determines the type of questions to reduce the size of answer space, as well as an answer cluster predictor that identifies the expected types of answers, such as object names, colors, and numbers. SCR [101] and HINT [102] employ a human attention-based penalty mechanism to guide the answer ranking. For each question-answer pair, SCR first determines the region of an image that has the greatest influence on the network prediction of the correct answer. Then, it penalizes the network for concentrating on the region once the prediction is wrong. Similarly, HINT penalizes the model if the pair-wise ranking of visual region sensitivities in relation to ground-truth answers does not match the rankings calculated from human-based attention maps. These two methods made significant progress using the human attention-based penalty mechanism, but Shrestha *et al.* [109] demonstrated that the performance improvements seen in these methods are due to a regularization effect that prevents overfitting to linguistic priors rather than enhanced visual grounding. Inspired by this, SimpleReg [109] employs

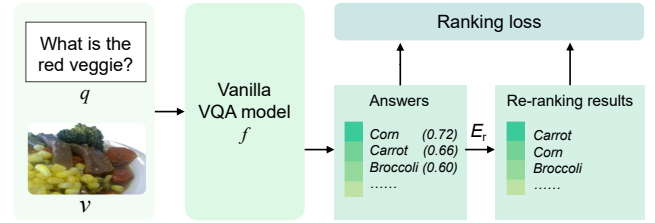


Fig. 14. Overview of answer re-ranking-based debiasing methods. The re-ranking module re-ranks the answers predicted by the vanilla VQA model.

a simple regularization scheme that consistently penalizes the model regardless of whether its predictions are accurate or not.

Different from the mentioned methods, RankVQA [108] and SAR [127] explore the combination of answer re-ranking and multimodality tasks to reduce bias learning. They first select candidate answers relevant to the question or the image, and then re-rank the answers by an image caption task [155], [156], [157] or a visual entailment task [158], [159], motivated by the idea that the correct answer must be more pertinent to the context of the image than the incorrect answer. These tasks play an important role in verifying whether the image semantically entails or matches the synthetic statement of questions and candidate answers.

The aforementioned methods mainly focus on strengthening the visual feature learning capability but ignore analyzing its inherent cause and providing an explicit interpretation. Therefore, some works [124], [128] suggested taking a look at the robust VQA problem from a class-imbalance perspective. They further demonstrated the effectiveness of the loss re-scaling strategy, which assigns various weights to each answer based on the statistics of the training data to estimate the final loss. For example, LPF [73] leverages a dynamic weighting scheme to each training example and adjusts the VQA loss according to the output distribution of a question-only branch. In addition, there are several works addressing bias learning from the perspective of decision margins. AdvQA [117], for example, employs an adapted margin loss function to distinguish between frequent and sparse answer spaces for each question type. RMLVQA [118] employs an instance-specific adaptive margin loss function to distinguish between hard and easy examples, as well as frequent and rare ones. MFE [110] employs a regularization

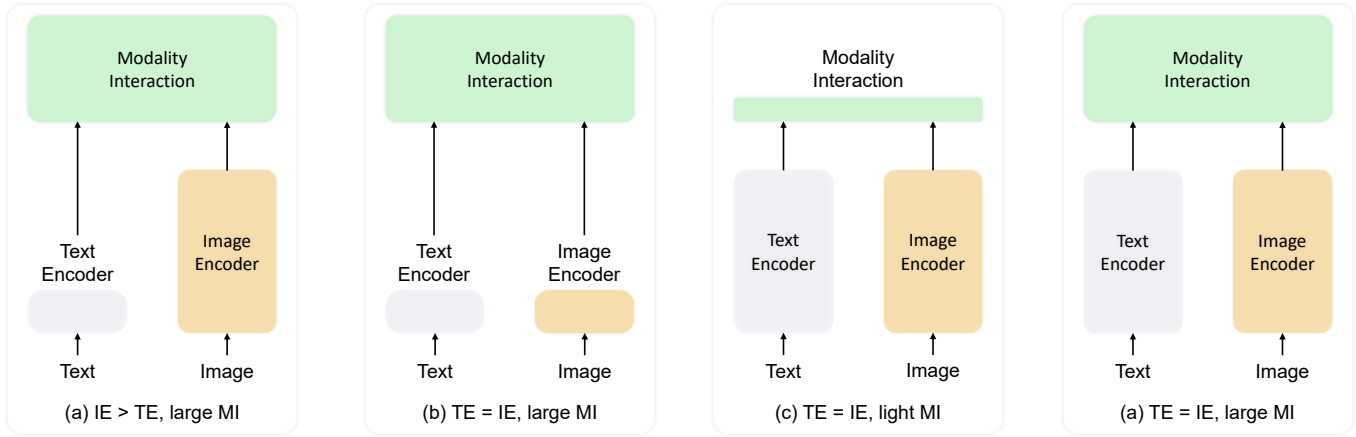


Fig. 15. Classification of VLP models inspired by [154]. The height of each rectangle represents its relative computational size. IE, TE, and MI are short for image encoder, text encoder, and modality interaction, respectively. In this paper, we consider the embedding layer as the component of encoders.

term that relies on a functional entropy, to ensure a balanced contribution of each modality towards classification.

## 6 VISION-AND-LANGUAGE PRE-TRAINING METHODS

The majority of approaches outlined previously are task-specific models that are trained on a restricted amount of data. However, there are other avenues worth exploring, such as task-agnostic models that are trained on vast amounts of data. Notably, in recent years, Vision-and-Language Pre-training (VLP) [47], [48], [81], [154], [160], [161], [162], [163], [164], [165], [166], [167], [168], [169], [170], [171] has seen significant advancements in the realm of multimodal representation learning through the use of large-scale image-text pairs. VLP models typically adopt Image-Text Matching (ITM) and Masked Language Modeling (MLM) objectives on images and their corresponding captions during pre-training and then are fine-tuned on downstream tasks such as VQA.

It is well-known that VLP models are usually more robust than the models trained on limited data [114], [172], [173]. Typically, VLP models consist of a text encoder, an image encoder, and a modality interaction module. Inspired by [154], we classify current VLP models into four categories based on the relative computational size of text encoders, image encoders, and modality interaction modules, as illustrated in Fig. 15. In this paper, we regard the embedding layer as the component of encoders. As a consensus, images usually contain more rich information than text, so intuitively, the encoder on the visual end should be larger than the encoder on the textual end. Furthermore, as a multimodal task, the interaction between modalities in VLP is also important, and the computational cost of the modality interaction module should not be sacrificed. Therefore, models of the third type empirically achieve worse performance than those of the other types [154].

During the initial phase of VLP, early methods such as LXMERT [81], UNITER [48], and OSCAR [162] employed object detectors like Faster R-CNN [174] and YOLO [175], which were pre-trained on the Visual Genome dataset [68],

as the visual encoder to extract region/object-level features from images. Therefore, the computational size of the image encoder exceeds that of the text encoder. Additionally, these methods utilize a deep Transformer to facilitate modality interactions, thus categorizing them into the first type, as illustrated in Fig. 15 (a). Although they demonstrate promising performance on downstream tasks, the use of heavy object detectors results in considerable computational expenses, and the inherently separate visual and textual embeddings pose a challenge for the modality interaction module to learn unified representations.

With the success of Transformer from natural language processing [176], [177], [178] to computer vision [179], [180], [181], researchers [182], [183], [184] paid attention to its use in VLP to address the separateness of visual and textual feature learning. For instance, inspired by the use of patches in ViT [179], ViLT [154] employs a light visual encoder where images are first split into patches and then embedded simply using a linear projection layer. These image features are then concatenated with word embeddings and fed into a deep Transformer for the modality interaction. The computational size of the text encoder is nearly equivalent to that of the image encoder, thus placing them within the second type, as illustrated in Fig. 15 (b). Compared to the VLP model with an object detector, ViLT’s convolution-free architecture significantly reduces model size and inference time, making it tens of times faster. However, the lightweight visual encoder of ViLT leads to a performance decrease on downstream tasks requiring salient visual features.

Meanwhile, CLIP [163] has shown great potential for training visual models using natural language supervision. This is achieved through an Image-Text Contrastive (ITC) objective, which determines whether an image and its corresponding caption are paired or not. With pre-training on a massive dataset of 400 million image-text pairs and the use of prompt templates, CLIP has achieved impressive results on various tasks [185], [186], [187], [188]. The modality interaction module only computes the ITC loss, making it classified as the third type, as shown in Fig. 15 (c). Although CLIP performs well on tasks such as image-text retrieval [189], it demonstrates limitations in handling other

TABLE 3

Results of VLP models on ID and OOD situations. The symbol PT indicates whether a method has been pre-trained on large-scale datasets. Results marked with †, ‡, ◊ are reported in [196], [128], [114], respectively. “DISC” denotes that methods regard VQA as a discriminative task, while “GEN” represents that methods consider VQA as a generative task. “Type” denotes the VLP class shown in Fig. 15.

Method	Type	PT	VQA-CP v2 test	VQA v2 validation	HM
UpDn [19]	-	No	37.81	65.99	48.07
VILBERT <sub>DISC</sub> <sup>†</sup> [160]	(a)	No	42.50	66.70	51.92
VILBERT <sub>DISC</sub> <sup>†</sup> [160]	(a)	Yes	42.90	67.00	52.31
ALBEF <sub>DISC</sub> <sup>†</sup> [164]	(a)	No	40.10	64.00	49.31
ALBEF <sub>DISC</sub> <sup>†</sup> (4M) [164]	(a)	Yes	44.40	70.00	54.34
ALBEF <sub>DISC</sub> <sup>†</sup> (14M) [164]	(a)	Yes	45.20	70.30	55.02
ALBEF <sub>GEN</sub> <sup>†</sup> [164]	(a)	No	36.60	61.40	45.86
ALBEF <sub>GEN</sub> <sup>†</sup> (4M) [164]	(a)	Yes	49.20	71.00	58.12
ALBEF <sub>GEN</sub> <sup>†</sup> (14M) [164]	(a)	Yes	49.60	72.10	58.77
UNITER <sub>Base</sub> <sup>◊</sup> [48]	(d)	Yes	46.93	72.70	57.04
UNITER <sub>Large</sub> <sup>◊</sup> [48]	(d)	Yes	50.98	73.82	60.31
LXMERT <sup>‡</sup> [81]	(d)	Yes	51.78	73.06	60.61
ViLT [154]	(b)	Yes	-	71.26	-
OSCAR [162]	(a)	Yes	-	73.61	-
CLIP-ViL [197]	(c)	Yes	-	76.48	-
BLIP [168]	(d)	Yes	-	78.25	-
BLIP-2 [171]	(d)	Yes	-	82.19	-
CoCa [167]	(d)	Yes	-	82.30	-
BEiT-3 [169]	(d)	Yes	-	84.19	-
PaLI [170]	(a)	Yes	-	84.30	-
PaLI-X [198]	(a)	Yes	-	86.00	-

important VLP tasks that involve finer-grained and more abstract concepts, such as fine-grained object detection [190], [191] and object counting in an image. This underscores the significance of the modality interaction module in achieving better performance on challenging VLP tasks.

Inspired by CLIP, some recent VLP works [192], [193], [194] explore pre-training based on contrastive learning. For instance, ALBEF [164] employs a 12-layer ViT and the first six layers of BERT as the image and text encoder, respectively. The representations learned by the mentioned encoder are aligned using the ITC loss. Following this alignment, the last six layers of BERT are employed as the multimodal encoder. Ultimately, the model is trained by jointly optimizing the ITC, ITM, and MLM losses. To learn from noisy data, ALBEF utilizes a momentum model [195] to generate pseudo-targets as additional supervision during training. ALBEF is a typical first-type model, which ensures that the image encoder is larger than the text encoder while also guaranteeing the expressiveness of the modality interaction module. Moreover, the abandonment of the pre-trained object detector and adoption of ViT with the ITC loss empowers ALBEF to acquire semantic visual representations of high quality, while maintaining computational efficiency.

The mentioned methods mainly employ the encoder-based architecture, while there is also another line of work adopting the encoder-decoder architecture. For instance, CoCa [167] replaces both the text and multimodal encoders with decoders and utilizes the Language Modeling (LM) loss for training. This approach improves training efficiency and achieves state-of-the-art results on a wide range of downstream tasks. BLIP [168] utilizes a multimodal mixture of encoder-decoder architecture, encompassing an image encoder, a text encoder, an image-grounded text encoder,

and an image-grounded text decoder. This comprehensive framework enables the integration of vision-language understanding and generation. The method undergoes joint pre-training with ITC, ITM, and LM losses, resulting in robust zero-shot generalization capabilities. Nevertheless, the cost associated with VLP has progressively become prohibitively high as a result of training large-scale models end-to-end. To address this issue, BLIP-2 [171] employs a lightweight querying Transformer to bridge the vision and language modality gap in two stages: vision-language representation learning from a frozen image encoder and vision-to-language generative learning from a frozen language model. Different from the above methods, BEiT-3 [169] seamlessly handles both text and images by treating images as a foreign language, such as “Imglsh”. This approach eliminates any inherent modeling differences and allows for a unified pretraining task [199], [200] known as mask-then-predict. Treating image-text pairs as “parallel sentences”, BEiT-3 effectively captures alignments between different modalities, obtaining transferable representations of considerable strength. All the aforementioned methods utilize high-computation-size encoders for images, text, and modality interactions, thereby classifying them within the fourth type, as depicted in Fig. 15 (d).

Table 3 shows the results of some VLP models on the VQA v2 validation (ID) and the VQA-CP v2 test (OOD) split. From the perspective of pre-training, it is evident that VLP yields significant improvements in both ID and OOD performance. For example, LXMERT outperforms UpDn by 13.97% and 7.07% on the mentioned split respectively. Notably, models with larger sizes demonstrate superior results in both scenarios. It can be seen that ALBEF<sub>DISC</sub> (14M) is superior to ALBEF<sub>DISC</sub> (4M) by 0.8% and 0.3% on ID and OOD situations respectively. In terms of modeling (answer obtaining), the generative model proves to be more robust compared to the discriminative model [196]. For instance, ALBEF<sub>GEN</sub> (4M) outperforms ALBEF<sub>DISC</sub> (4M) by 4.8% and 1.0% on the mentioned split respectively. Furthermore, the considerable gap between ID and OOD performance indicates ample room for further improvement in VLP models. Specifically, in the case of LXMERT, this difference is quantified as 21.28%, highlighting the considerable scope for improvement in bridging this gap.

## 7 DISCUSSIONS AND FUTURE DIRECTIONS

Based on the comprehensive analysis of existing datasets, evaluations, and methods outlined above, it becomes apparent that there is potential for improvement in robust VQA. Consequently, our focus will now shift toward discussing the strategies and areas where future advancements can be made.

**Does the dataset annotation exhibit a high level of quality?** Most of the existing datasets were developed based on the VQA v2 dataset [12]. However, the answer annotations in the dataset often lack consistent agreement, which can result in inaccurate evaluation outcomes. For instance, as illustrated in Fig. 3, a system that generates a “Yes” or “No” answer for the “Yes/No” question would receive an accuracy score of “1.00” or “0.67”, respectively. Therefore,

TABLE 4

The accuracy (%) comparison of non-debiasing (ND) and debiasing (DE) methods on various datasets. All the results are on the test split except for the result of the VQA v2.0 testdev split.

Type	Backbone	Methods	VQA v2.0 test-dev				VQA-CP v1 test				VQA-CP v2 test				GQA-OOD val		
			All	Y/N	Num.	Other	All	Y/N	Num.	Other	All	Y/N	Num.	Other	All	Tail	Head
NDE	NA	SMRL	64.76	82.20	46.44	54.01	36.86	43.39	12.88	40.22	37.09	41.85	12.76	41.28	46.32	41.67	49.16
		UpDn	65.78	83.07	45.88	55.54	37.40	43.27	12.89	41.57	38.04	43.41	12.92	42.26	47.75	42.62	50.89
DE	SMRL	CF Variant	62.63	82.14	44.02	50.14	43.76	60.83	13.92	38.92	54.04	88.23	30.86	42.71	39.34	35.09	41.95
		RUBi	63.28	82.28	45.46	51.05	50.83	80.18	16.52	39.43	47.61	74.68	20.31	43.23	46.78	42.52	49.39
	CF	63.01	81.96	45.48	50.98	56.88	89.75	17.56	40.21	55.42	90.56	26.61	45.65	44.28	41.20	44.28	
	UpDn	CF Variant	65.19	82.98	44.93	54.58	37.26	44.99	13.08	41.68	37.59	44.04	13.03	41.97	48.03	44.21	50.38
		RUBi	64.94	83.22	45.51	53.71	50.45	80.25	14.76	41.01	39.57	49.74	19.17	42.38	48.03	42.24	51.59
		CF	65.47	83.16	44.72	55.07	57.64	89.18	14.57	43.75	54.02	91.35	13.46	45.60	45.24	41.11	47.78

current data quality cannot support the accurate performance measurement of VQA models. In the future, we should ensure the quality of data annotations [201], such as introducing a process where annotations are reviewed by experienced annotators or experts for ambiguous cases.

**What datasets should be developed?** Although existing datasets, especially the OOD dataset, enable us to provide insight into the robustness of VQA methods [202], [203], it is essential to note that each dataset has its own unique limitations. Taking the most commonly used OOD dataset VQA-CP [29] as an example, it has two shortcomings. First, its distribution between training and test splits is significantly different or even reversed, which may not align with the real-world scenario. Some methods [29], [34], [72] may be devised based on this prior, which may not reflect the robustness of these methods accurately. Second, VQA-CP lacks the validation split, which results in methods being tuned on the test split. Although GQA-OOD [36] alleviates the above issues, its test split is too small, only containing 12,578 questions. *Therefore, existing datasets may not be sufficient to evaluate robustness. Furthermore, the dataset does not involve fine-grained bias evaluations such as vision shortcut measurement. To address this issue, we should develop a dataset that satisfies the following properties in the future.*

- The dataset should be sufficiently large and complete, with adequate validation splits for fine-tuning hyper-parameters and large splits for training and testing.
- The dataset should contain ID and OOD test settings simultaneously. In this way, we can conduct a comprehensive and fair evaluation of the robustness of VQA methods.
- The distribution between training and test splits should be more natural, rather than artificially setting significantly different or even contradictory data distributions. The artificial distribution prior may be used to improve model performance, while the prior can not be applied to other situations, leading to poor generalization ability.
- The OOD test setting should simultaneously include language, vision, and multimodality bias, to have a more refined assessment of robustness.
- The question format should be various, particularly in the test split. The question in existing datasets is usually generated by the template. However, the question patterns generated by templates may be

not enough, and be learned or memorized easily, resulting in inaccurate comparisons.

**Are the evaluation metrics effective enough?** Current evaluation protocols assign equal weight to each question. However, some questions, such as the OOD question requiring multi-hop reasoning, should be treated as more important. Therefore, in the future, we should devise an evaluation protocol that can assign different weights to questions according to annotations, such as the distribution they belong to and their difficulty. Furthermore, only accuracy is typically used to evaluate the robustness of methods, which may not be sufficient. In the future, we may apply composite metrics such as “validity” and “plausibility” [15] to evaluate VQA methods from various angles.

**Are the existing debiasing methods robust enough?** A variety of debiasing methods [35], [78], [89] for VQA have been proposed and have achieved significant success on VQA v2 and VQA-CP which are the most commonly used datasets to evaluate robustness. This inspires us to consider whether they are robust to other datasets, such as GQA-OOD. To address our curiosity, we select several non-debiasing methods, including SMRL [20] and UpDn [19], and debiasing methods, including RUBi [34] and CF [120], and then conduct experiments on these three datasets simultaneously for a fair comparison. The results are shown in Table 4. It can be seen that existing debiasing methods are backbone-sensitive and cannot achieve ongoing success on other datasets. For instance, when using the CF Variant with SMRL, an accuracy of 43.76% is achieved on the VQA-CP v1 dataset. In contrast, when employing the CF variant with UpDn, the accuracy drops to 37.26%. Additionally, CF with UpDn attains an accuracy of 45.24% on the GQA-OOD validation split, which is 2.51% lower than that of UpDn alone. We can also note that current debiasing methods still achieve high OOD performance at the expense of ID performance. Specifically, RUBi with SMRL obtains the improvement of 0.46% on the GQA-OOD validation split, while it drops by 0.48% on the VQA v2.0 test-dev split. These show that we should develop true robust methods in the future to perform well in a variety of ID and OOD performances at the same time.

**Are the existing VLP methods robust enough?** In recent years, VLP models have gained significant attention and achieved remarkable success across various tasks [204], establishing themselves as a prominent research area. Table 3 presents the performance of representative VLP methods on

the VQA-CP v2 test split and the VQA v2 validation split. Notably, early VLP methods like UNITER and LXMERT exhibit a certain degree of robustness, but there remains room for improvement, especially in reducing the performance gap between ID and OOD situations. Moreover, there appears to be limited research exploring the robustness of more recent VLP models such as BEiT-3 and PaLI on VQA-CP and GQA-OOD. We think that exploring the robustness of these newer models could be an intriguing direction for future research.

### How should we verify the robustness of the method?

Existing works frequently employ VQA v2 and VQA-CP to assess both debiasing methods and VLP methods. These methods, however, do not perform well on the other OOD datasets, as shown in Table 4. Therefore, considering current dataset conditions, we should leverage multiple ID and OOD datasets to verify the robustness simultaneously, which can reflect the robustness more comprehensively and accurately.

## 8 CONCLUSION

This paper presents a comprehensive survey that focuses on the domain of robust Visual Question Answering (VQA). We conduct a systematic review of existing datasets from ID and OOD angles, evaluation metrics from the single and composite views, and methods from the perspective of debiasing techniques. Specifically, we classify the existing debiasing methods into four categories: ensemble learning, data augmentation, self-supervised contrastive learning, and answer re-ranking. We review the robustness of vision-and-language pre-training methods on VQA, classifying them into four categories according to the relative computational size of text encoders, image encoders, and modality interaction modules. We discuss future research directions that should be prioritized for robust VQA.

## ACKNOWLEDGMENTS

This work was supported by the National Key Research and Development Program of China (2021YFB1715600), the National Natural Science Foundation of China (U22B2019, 62272372, 62293553, 62250066, 621737002).

## REFERENCES

- [1] S. Antol, A. Agrawal, J. Lu, M. Mitchell, D. Batra, C. L. Zitnick, and D. Parikh, "Vqa: Visual question answering," in *ICCV*, 2015, pp. 2425–2433.
- [2] K. Kafle and C. Kanan, "Visual question answering: Datasets, algorithms and future challenges," *CVIU*, vol. 163, pp. 3–20, 2017.
- [3] N. Liu, Q. Pu, Y. Shi, S. Zhang, and L. Qiu, "Older adults' interaction with intelligent virtual assistants: the role of information modality and feedback," *IJHCS*, vol. 39, no. 5, pp. 1162–1183, 2023.
- [4] E. Zangerle and C. Bauer, "Evaluating recommender systems: Survey and framework," *ACM Computing Surveys*, vol. 55, no. 8, pp. 1–38, 2022.
- [5] L. Chen, Y. Li, C. Huang, B. Li, Y. Xing, D. Tian, L. Li, Z. Hu, X. Na, Z. Li *et al.*, "Milestones in autonomous driving and intelligent vehicles: Survey of surveys," *IEEE TIV*, vol. 8, no. 2, pp. 1046–1056, 2022.
- [6] S. Whitehead, H. Wu, H. Ji, R. Feris, and K. Saenko, "Separating skills and concepts for novel visual question answering," in *CVPR*, 2021, pp. 5632–5641.
- [7] Y. Liu, X. Zhang, Q. Zhang, C. Li, F. Huang, X. Tang, and Z. Li, "Dual self-attention with co-attention networks for visual question answering," *PR*, vol. 117, p. 107956, 2021.
- [8] J. Park, J. Lee, and K. Sohn, "Bridge to answer: Structure-aware graph interaction network for video question answering," in *CVPR*, 2021, pp. 15 526–15 535.
- [9] T. Rahman, S.-H. Chou, L. Sigal, and G. Carenini, "An improved attention for visual question answering," in *CVPR*, 2021, pp. 1653–1662.
- [10] Q. Cao, X. Liang, B. Li, and L. Lin, "Interpretable visual question answering by reasoning on dependency trees," *IEEE TPAMI*, vol. 43, no. 3, pp. 887–901, 2019.
- [11] J. Cao, X. Qin, S. Zhao, and J. Shen, "Bilateral cross-modality graph matching attention for feature fusion in visual question answering," *IEEE TNNLS*, 2022.
- [12] Y. Goyal, T. Khot, D. Summers-Stay, D. Batra, and D. Parikh, "Making the v in vqa matter: Elevating the role of image understanding in visual question answering," in *CVPR*, 2017, pp. 6904–6913.
- [13] P. Wang, Q. Wu, C. Shen, A. Dick, and A. Van Den Hengel, "Fvqa: Fact-based visual question answering," *IEEE TPAMI*, vol. 40, no. 10, pp. 2413–2427, 2017.
- [14] K. Marino, M. Rastegari, A. Farhadi, and R. Mottaghi, "Ok-vqa: A visual question answering benchmark requiring external knowledge," in *CVPR*, 2019, pp. 3195–3204.
- [15] D. A. Hudson and C. D. Manning, "Gqa: A new dataset for real-world visual reasoning and compositional question answering," in *CVPR*, 2019, pp. 6700–6709.
- [16] A. Fukui, D. H. Park, D. Yang, A. Rohrbach, T. Darrell, and M. Rohrbach, "Multimodal compact bilinear pooling for visual question answering and visual grounding," in *EMNLP*, 2016, pp. 457–468.
- [17] L. Ma, Z. Lu, and H. Li, "Learning to answer questions from image using convolutional neural network," in *AAAI*, 2016, pp. 3567–3573.
- [18] Z. Yang, X. He, J. Gao, L. Deng, and A. Smola, "Stacked attention networks for image question answering," in *CVPR*, 2016, pp. 21–29.
- [19] P. Anderson, X. He, C. Buehler, D. Teney, M. Johnson, S. Gould, and L. Zhang, "Bottom-up and top-down attention for image captioning and visual question answering," in *CVPR*, 2018, pp. 6077–6086.
- [20] R. Cadene, H. Ben-Younes, M. Cord, and N. Thome, "Murel: Multimodal relational reasoning for visual question answering," in *CVPR*, 2019, pp. 1989–1998.
- [21] P. Gao, Z. Jiang, H. You, P. Lu, S. C. Hoi, X. Wang, and H. Li, "Dynamic fusion with intra-and inter-modality attention flow for visual question answering," in *CVPR*, 2019, pp. 6639–6648.
- [22] J. Wu, J. Lu, A. Sabharwal, and R. Mottaghi, "Multi-modal answer validation for knowledge-based vqa," in *AAAI*, 2022, pp. 2712–2721.
- [23] Y. Ding, J. Yu, B. Liu, Y. Hu, M. Cui, and Q. Wu, "Mukeya: Multimodal knowledge extraction and accumulation for knowledge-based visual question answering," in *CVPR*, 2022, pp. 5089–5098.
- [24] S. Ravi, A. Chinchure, L. Sigal, R. Liao, and V. Shwartz, "Vlc-bert: Visual question answering with contextualized commonsense knowledge," in *WACV*, 2023, pp. 1155–1165.
- [25] S. Auer, C. Bizer, G. Kobilarov, J. Lehmann, R. Cyganiak, and Z. Ives, "Dbpedia: A nucleus for a web of open data," in *ISWC-ASWC*, 2007, pp. 722–735.
- [26] K. Bollacker, C. Evans, P. Paritosh, T. Sturge, and J. Taylor, "Freebase: A collaboratively created graph database for structuring human knowledge," in *SIGMOD*, 2008, pp. 1247–1250.
- [27] J. Hoffart, F. M. Suchanek, K. Berberich, and G. Weikum, "Yago2: A spatially and temporally enhanced knowledge base from wikipedia," *Artificial intelligence*, vol. 194, pp. 28–61, 2013.
- [28] T. Baltrušaitis, C. Ahuja, and L.-P. Morency, "Multimodal machine learning: A survey and taxonomy," *IEEE TPAMI*, vol. 41, no. 2, pp. 423–443, 2019.
- [29] A. Agrawal, D. Batra, D. Parikh, and A. Kembhavi, "Don't just assume; look and answer: Overcoming priors for visual question answering," in *CVPR*, 2018, pp. 4971–4980.
- [30] Y. Niu and H. Zhang, "Introspective distillation for robust question answering," in *NeurIPS*, 2021, pp. 16 292–16 304.
- [31] J. M. Kim, A. S. Koepke, C. Schmid, and Z. Akata, "Exposing and mitigating spurious correlations for cross-modal retrieval," in *CVPR Workshop*, June 2023, pp. 2584–2594.

- [32] X. Zhang, F. Zhang, and C. Xu, "Next-ood: Overcoming dual multiple-choice vqa biases," *IEEE TPAMI*, 2023.
- [33] Y. Song, X. Yang, Y. Wang, and C. Xu, "Recovering generalization via pre-training-like knowledge distillation for out-of-distribution visual question answering," *IEEE TMM*, 2023.
- [34] R. Cadene, C. Dancette, H. Ben-younes, M. Cord, and D. Parikh, "Rubi: Reducing unimodal biases for visual question answering," in *NeurIPS*, 2019, pp. 841–852.
- [35] V. Gupta, Z. Li, A. Kortylewski, C. Zhang, Y. Li, and A. Yuille, "Swapmix: Diagnosing and regularizing the over-reliance on visual context in visual question answering," in *CVPR*, 2022, pp. 5078–5088.
- [36] C. Kervadec, G. Antipov, M. Baccouche, and C. Wolf, "Roses are red, violets are blue... but should vqa expect them to?" in *CVPR*, 2021, pp. 2776–2785.
- [37] Q. Si, F. Meng, M. Zheng, Z. Lin, Y. Liu, P. Fu, Y. Cao, W. Wang, and J. Zhou, "Language prior is not the only shortcut: A benchmark for shortcut learning in vqa," in *Findings of EMNLP*, 2022, pp. 3698–3712.
- [38] K. Kafle and C. Kanan, "An analysis of visual question answering algorithms," in *ICCV*, 2017, pp. 1965–1973.
- [39] Q. Wu, C. Shen, P. Wang, A. Dick, and A. Van Den Hengel, "Image captioning and visual question answering based on attributes and external knowledge," *IEEE TPAMI*, vol. 40, no. 6, pp. 1367–1381, 2017.
- [40] W. Guo, Y. Zhang, J. Yang, and X. Yuan, "Re-attention for visual question answering," *IEEE TIP*, vol. 30, pp. 6730–6743, 2021.
- [41] T. Wolf, L. Debut, V. Sanh, J. Chaumond, C. Delangue, A. Moi, P. Cistac, T. Rault, R. Louf, M. Funtowicz *et al.*, "Transformers: State-of-the-art natural language processing," in *EMNLP*, 2020, pp. 38–45.
- [42] T. Naseem, S. Ravishankar, N. Mihindukulasooriya, I. Abdelaziz, Y.-S. Lee, P. Kapanipathi, S. Roukos, A. Gliozzo, and A. Gray, "A semantics-aware transformer model of relation linking for knowledge base question answering," in *ACL-IJCNN*, 2021, pp. 256–262.
- [43] S. Garg, T. Vu, and A. Moschitti, "Tanda: Transfer and adapt pre-trained transformer models for answer sentence selection," in *AAAI*, 2020, pp. 7780–7788.
- [44] M. Glass, A. Gliozzo, R. Chakravarti, A. Ferritto, G. S. Bhargav, D. Garg, A. Sil, and L. Pan, "Span selection pre-training for question answering," in *ACL*, 2020.
- [45] Z. Zhang, Y. Wu, J. Zhou, S. Duan, H. Zhao, and R. Wang, "Sg-net: Syntax guided transformer for language representation," *IEEE TPAMI*, vol. 44, no. 06, pp. 3285–3299, 2020.
- [46] Y. Zhou, L. Liao, Y. Gao, R. Wang, and H. Huang, "Topicbert: A topic-enhanced neural language model fine-tuned for sentiment classification," *IEEE TNNLS*, 2021.
- [47] L. H. Li, M. Yatskar, D. Yin, C.-J. Hsieh, and K.-W. Chang, "Visualbert: A simple and performant baseline for vision and language," *arXiv preprint arXiv:1908.03557*, 2019.
- [48] Y.-C. Chen, L. Li, L. Yu, A. El Kholly, F. Ahmed, Z. Gan, Y. Cheng, and J. Liu, "Uniter: Universal image-text representation learning," in *ECCV*, 2020, pp. 104–120.
- [49] G. Li, N. Duan, Y. Fang, M. Gong, and D. Jiang, "Unicoder-vl: A universal encoder for vision and language by cross-modal pre-training," in *AAAI*, 2020, pp. 11 336–11 344.
- [50] Z. Yang, T. Luo, D. Wang, Z. Hu, J. Gao, and L. Wang, "Learning to navigate for fine-grained classification," in *ECCV*, 2018, pp. 420–435.
- [51] S. Zhao, Z. Wen, Q. Qi, K.-M. Lam, and J. Shen, "Learning fine-grained information with capsule-wise attention for salient object detection," *IEEE TMM*, 2023.
- [52] Z.-J. Zha, D. Liu, H. Zhang, Y. Zhang, and F. Wu, "Context-aware visual policy network for fine-grained image captioning," *IEEE TPAMI*, vol. 44, no. 2, pp. 710–722, 2019.
- [53] H. Zhao, J. Jia, and V. Koltun, "Exploring self-attention for image recognition," in *CVPR*, 2020, pp. 10 076–10 085.
- [54] C. Xie, M. Tan, B. Gong, J. Wang, A. L. Yuille, and Q. V. Le, "Adversarial examples improve image recognition," in *CVPR*, 2020, pp. 819–828.
- [55] J. Chen, M. Jiang, Q. Dou, and Q. Chen, "Federated domain generalization for image recognition via cross-client style transfer," in *WACV*, 2023, pp. 361–370.
- [56] M. Acharya, K. Kafle, and C. Kanan, "Tallyqa: Answering complex counting questions," in *AAAI*, 2019, pp. 8076–8084.
- [57] V. A. Sindagi and V. M. Patel, "Ha-ccn: Hierarchical attention-based crowd counting network," *IEEE TIP*, vol. 29, pp. 323–335, 2019.
- [58] T.-Y. Lin, M. Maire, S. Belongie, J. Hays, P. Perona, D. Ramanan, P. Dollár, and C. L. Zitnick, "Microsoft coco: Common objects in context," in *ECCV*, 2014, pp. 740–755.
- [59] H. Jiang, I. Misra, M. Rohrbach, E. Learned-Miller, and X. Chen, "In defense of grid features for visual question answering," in *CVPR*, 2020, pp. 10 267–10 276.
- [60] L. Li, Z. Gan, Y. Cheng, and J. Liu, "Relation-aware graph attention network for visual question answering," in *ICCV*, 2019, pp. 10 313–10 322.
- [61] J. Ma, J. Liu, Q. Lin, B. Wu, Y. Wang, and Y. You, "Multitask learning for visual question answering," *IEEE TNNLS*, vol. 34, no. 3, pp. 1380–1394, 2023.
- [62] B. X. Nguyen, T. Do, H. Tran, E. Tjiputra, Q. D. Tran, and A. Nguyen, "Coarse-to-fine reasoning for visual question answering," in *CVPR*, 2022, pp. 4558–4566.
- [63] G. Luo, Y. Zhou, X. Sun, Y. Wang, L. Cao, Y. Wu, F. Huang, and R. Ji, "Towards lightweight transformer via group-wise transformation for vision-and-language tasks," *IEEE TIP*, vol. 31, pp. 3386–3398, 2022.
- [64] D. Rosenberg, I. Gat, A. Feder, and R. Reichart, "Are vqa systems red? measuring robustness to augmented data with focused interventions," in *ACL-IJCNLP*, 2021, pp. 61–70.
- [65] P. Zhang, Y. Goyal, D. Summers-Stay, D. Batra, and D. Parikh, "Yin and yang: Balancing and answering binary visual questions," in *CVPR*, 2016, pp. 5014–5022.
- [66] A. Das, H. Agrawal, L. Zitnick, D. Parikh, and D. Batra, "Human attention in visual question answering: Do humans and deep networks look at the same regions?" *CVIU*, vol. 163, pp. 90–100, 2017.
- [67] J. Johnson, B. Hariharan, L. Van Der Maaten, L. Fei-Fei, C. Lawrence Zitnick, and R. Girshick, "Clevr: A diagnostic dataset for compositional language and elementary visual reasoning," in *CVPR*, 2017, pp. 2901–2910.
- [68] R. Krishna, Y. Zhu, O. Groth, J. Johnson, K. Hata, J. Kravitz, S. Chen, Y. Kalantidis, L.-J. Li, D. A. Shamma *et al.*, "Visual genome: Connecting language and vision using crowdsourced dense image annotations," *IJCV*, vol. 123, no. 1, pp. 32–73, 2017.
- [69] B. Thomee, D. A. Shamma, G. Friedland, B. Elizalde, K. Ni, D. Poland, D. Borth, and L.-J. Li, "Yfcc100m: The new data in multimedia research," *Communications of the ACM*, vol. 59, no. 2, pp. 64–73, 2016.
- [70] P. Zhang, X. Li, X. Hu, J. Yang, L. Zhang, L. Wang, Y. Choi, and J. Gao, "Vinvl: Revisiting visual representations in vision-language models," in *CVPR*, 2021, pp. 5579–5588.
- [71] D. Gao, R. Wang, S. Shan, and X. Chen, "Cric: A vqa dataset for compositional reasoning on vision and commonsense," *IEEE TPAMI*, pp. 1–18, 2022.
- [72] M. Lao, Y. Guo, Y. Liu, W. Chen, N. Pu, and M. S. Lew, "From superficial to deep: Language bias driven curriculum learning for visual question answering," in *ACM MM*, 2021, pp. 3370–3379.
- [73] Z. Liang, H. Hu, and J. Zhu, "Lpf: A language-prior feedback objective function for de-biased visual question answering," in *SIGIR*, 2021, pp. 1955–1959.
- [74] J. W. Cho, D.-J. Kim, H. Ryu, and I. S. Kweon, "Generative bias for robust visual question answering," in *CVPR*, 2023, pp. 11 681–11 690.
- [75] A. Basu, S. Addepalli, and R. V. Babu, "Rmlvqa: A margin loss approach for visual question answering with language biases," in *CVPR*, 2023, pp. 11 671–11 680.
- [76] M. Shah, X. Chen, M. Rohrbach, and D. Parikh, "Cycle-consistency for robust visual question answering," in *CVPR*, 2019, pp. 6642–6651.
- [77] C. Dancette, R. Cadene, D. Teney, and M. Cord, "Beyond question-based biases: Assessing multimodal shortcut learning in visual question answering," in *ICCV*, 2021, pp. 1554–1563.
- [78] L. Li, J. Lei, Z. Gan, and J. Liu, "Adversarial vqa: A new benchmark for evaluating the robustness of vqa models," in *ICCV*, 2021, pp. 2022–2031.
- [79] V. Agarwal, R. Shetty, and M. Fritz, "Towards causal vqa: Revealing and reducing spurious correlations by invariant and covariant semantic editing," in *CVPR*, 2020, pp. 9690–9698.
- [80] T. Gokhale, P. Banerjee, C. Baral, and Y. Yang, "Vqa-lol: Visual question answering under the lens of logic," in *ECCV*, 2020, pp. 379–396.



- [81] H. Tan and M. Bansal, "Lxmert: Learning cross-modality encoder representations from transformers," in *EMNLP-IJCNLP*, 2019, pp. 5100–5111.
- [82] M. Malinowski and M. Fritz, "A multi-world approach to question answering about real-world scenes based on uncertain input," in *NeurIPS*, 2014, pp. 1682–1690.
- [83] H. Gao, J. Mao, J. Zhou, Z. Huang, L. Wang, and W. Xu, "Are you talking to a machine? dataset and methods for multilingual image question answering," in *NeurIPS*, 2015, pp. 2296–2304.
- [84] Y. Zhu, O. Groth, M. Bernstein, and L. Fei-Fei, "Visual7w: Grounded question answering in images," in *CVPR*, 2016, pp. 4995–5004.
- [85] P. Sharma, N. Ding, S. Goodman, and R. Soicrut, "Conceptual captions: A cleaned, hypertexted, image alt-text dataset for automatic image captioning," in *ACL*, 2018, pp. 2556–2565.
- [86] N. Kai, L. Sharon, and Y. W. William, "Fakeddit: A new multi-modal benchmark dataset for fine-grained fake news detection," in *LREC*, 2020, pp. 6149–6157.
- [87] S. Sheng, A. Singh, V. Goswami, J. Magana, T. Thrush, W. Galuba, D. Parikh, and D. Kiela, "Human-adversarial visual question answering," in *NeurIPS*, 2021, pp. 20 346–20 359.
- [88] D. Kiela, M. Bartolo, Y. Nie, D. Kaushik, A. Geiger, Z. Wu, B. Vidgen, G. Prasad, A. Singh, P. Ringshia *et al.*, "Dynabench: Rethinking benchmarking in nlp," in *NAACL*, 2021, pp. 4110–4124.
- [89] Z. Liang, W. Jiang, H. Hu, and J. Zhu, "Learning to contrast the counterfactual samples for robust visual question answering," in *EMNLP*, 2020, pp. 3285–3292.
- [90] L. Chen, X. Yan, J. Xiao, H. Zhang, S. Pu, and Y. Zhuang, "Counterfactual samples synthesizing for robust visual question answering," in *CVPR*, 2020, pp. 10797–10806.
- [91] M. Lao, Y. Guo, W. Chen, N. Pu, and M. S. Lew, "Vqa-bc: Robust visual question answering via bidirectional chaining," in *ICASSP*, 2022, pp. 4833–4837.
- [92] H. Lancaster and E. Seneta, "Chi-square distribution. encyclopedia of biostatistics," 2005.
- [93] A. Agrawal, D. Batra, and D. Parikh, "Analyzing the behavior of visual question answering models," in *EMNLP*, 2016, pp. 1955–1960.
- [94] J.-H. Kim, J. Jun, and B.-T. Zhang, "Bilinear attention networks," in *NeurIPS*, 2018, pp. 1571–1581.
- [95] J. Jiang, Z. Liu, Y. Liu, Z. Nan, and N. Zheng, "X-ggm: Graph generative modeling for out-of-distribution generalization in visual question answering," in *ACM MM*, 2021, pp. 199–208.
- [96] M. Qraitem, K. Saenko, and B. A. Plummer, "Bias mimicking: A simple sampling approach for bias mitigation," in *CVPR*, 2023, pp. 20 311–20 320.
- [97] G. E. Hinton, "Training products of experts by minimizing contrastive divergence," *Neural Computation*, vol. 14, no. 8, pp. 1771–1800, 2002.
- [98] K. Kafle, M. Yousefhusien, and C. Kanan, "Data augmentation for visual question answering," in *INLG*, 2017, pp. 198–202.
- [99] J. Kil, C. Zhang, D. Xuan, and W.-L. Chao, "Discovering the unknown knowns: Turning implicit knowledge in the dataset into explicit training examples for visual question answering," in *EMNLP*, 2021, pp. 6346–6361.
- [100] S. Ramakrishnan, A. Agrawal, and S. Lee, "Overcoming language priors in visual question answering with adversarial regularization," in *NeurIPS*, 2018, pp. 1548–1558.
- [101] J. Wu and R. Mooney, "Self-critical reasoning for robust visual question answering," *NeurIPS*, p. 8601–8611, 2019.
- [102] R. R. Selvaraju, S. Lee, Y. Shen, H. Jin, S. Ghosh, L. Heck, D. Batra, and D. Parikh, "Taking a hint: Leveraging explanations to make vision and language models more grounded," in *ICCV*, 2019, pp. 2591–2600.
- [103] C. Clark, M. Yatskar, and L. Zettlemoyer, "Don't take the easy way out: Ensemble based methods for avoiding known dataset biases," in *EMNLP*, 2019, pp. 4069–4082.
- [104] D. Teney and A. v. d. Hengel, "Actively seeking and learning from live data," in *CVPR*, 2019, pp. 1940–1949.
- [105] C. Jing, Y. Wu, X. Zhang, Y. Jia, and Q. Wu, "Overcoming language priors in vqa via decomposed linguistic representations," in *AAAI*, 2020, pp. 11 181–11 188.
- [106] E. Abbasnejad, D. Teney, A. Parvaneh, J. Shi, and A. v. d. Hengel, "Counterfactual vision and language learning," in *CVPR*, 2020, pp. 10 044–10 054.
- [107] D. Teney, E. Abbasnejad, and A. van den Hengel, "Learning what makes a difference from counterfactual examples and gradient supervision," in *ECCV*, 2020, pp. 580–599.
- [108] Y. Qiao, Z. Yu, and J. Liu, "Rankvqa: Answer re-ranking for visual question answering," in *ICME*, 2020, pp. 1–6.
- [109] R. Shrestha, K. Kafle, and C. Kanan, "A negative case analysis of visual grounding methods for vqa," in *ACL*, 2020, pp. 8172–8181.
- [110] I. Gat, I. Schwartz, A. Schwing, and T. Hazan, "Removing bias in multi-modal classifiers: Regularization by maximizing functional entropies," in *NeurIPS*, 2020, pp. 3197–3208.
- [111] G. Kv and A. Mittal, "Reducing language biases in visual question answering with visually-grounded question encoder," in *ECCV*, 2020, pp. 18–34.
- [112] D. Teney, K. Kafle, R. Shrestha, E. Abbasnejad, C. Kanan, and A. van den Hengel, "On the value of out-of-distribution testing: An example of goodhart's law," in *NeurIPS*, 2020, pp. 407–417.
- [113] Z. Gan, Y.-C. Chen, L. Li, C. Zhu, Y. Cheng, and J. Liu, "Large-scale adversarial training for vision-and-language representation learning," *NeurIPS*, pp. 6616–6628, 2020.
- [114] L. Li, Z. Gan, and J. Liu, "A closer look at the robustness of vision-and-language pre-trained models," *arXiv:2012.08673*, 2020.
- [115] T. Gokhale, P. Banerjee, C. Baral, and Y. Yang, "Mutant: A training paradigm for out-of-distribution generalization in visual question answering," in *EMNLP*, 2020, pp. 878–892.
- [116] C. Clark, M. Yatskar, and L. Zettlemoyer, "Learning to model and ignore dataset bias with mixed capacity ensembles," in *Findings of EMNLP*, 2020, pp. 3031–3045.
- [117] Y. Guo, L. Nie, Z. Cheng, F. Ji, J. Zhang, and A. D. Bimbo, "Adavqa: Overcoming language priors with adapted margin cosine loss," in *IJCAI*, 2021, pp. 708–714.
- [118] A. Basu, S. Addepalli, and R. V. Babu, "Rmlvqa: A margin loss approach for visual question answering with language biases," in *CVPR*, 2023, pp. 11 671–11 680.
- [119] D. Teney, E. Abbasnejad, and A. van den Hengel, "Unshuffling data for improved generalization in visual question answering," in *ICCV*, 2021, pp. 1417–1427.
- [120] Y. Niu, K. Tang, H. Zhang, Z. Lu, X.-S. Hua, and J.-R. Wen, "Counterfactual vqa: A cause-effect look at language bias," in *CVPR*, 2021, pp. 12700–12710.
- [121] Y. Pan, Z. Li, L. Zhang, and J. Tang, "Distilling knowledge in causal inference for unbiased visual question answering," in *MMAsia*, 2021, pp. 1–7.
- [122] X. Han, S. Wang, C. Su, Q. Huang, and Q. Tian, "Greedy gradient ensemble for robust visual question answering," in *ICCV*, 2021, pp. 1584–1593.
- [123] C. Yang, S. Feng, D. Li, H. Shen, G. Wang, and B. Jiang, "Learning content and context with language bias for visual question answering," in *ICME*, 2021, pp. 1–6.
- [124] M. Lao, Y. Guo, Y. Liu, and M. S. Lew, "A language prior based focal loss for visual question answering," in *ICME*, 2021, pp. 1–6.
- [125] X. Zhu, Z. Mao, C. Liu, P. Zhang, B. Wang, and Y. Zhang, "Overcoming language priors with self-supervised learning for visual question answering," in *IJCAI*, 2021, pp. 1083–1089.
- [126] Z. Wen, G. Xu, M. Tan, Q. Wu, and Q. Wu, "Debiased visual question answering from feature and sample perspectives," in *NeurIPS*, 2021, pp. 3784–3796.
- [127] Q. Si, Z. Lin, M. yu Zheng, P. Fu, and W. Wang, "Check it again: Progressive visual question answering via visual entailment," in *ACL*, 2021, pp. 4101–4110.
- [128] Y. Guo, L. Nie, Z. Cheng, Q. Tian, and M. Zhang, "Loss re-scaling vqa: Revisiting the language prior problem from a class-imbalance view," *IEEE TIP*, pp. 227–238, 2022.
- [129] C. Kolling, M. More, N. Gavenski, E. Pooch, O. Parraga, and R. C. Barros, "Efficient counterfactual debiasing for visual question answering," in *WACV*, 2022, pp. 3001–3010.
- [130] Q. Si, Y. Liu, F. Meng, Z. Lin, P. Fu, Y. Cao, W. Wang, and J. Zhou, "Towards robust visual question answering: Making the most of biased samples via contrastive learning," in *Findings of EMNLP*, 2022, pp. 6650–6662.
- [131] L. Chen, Y. Zheng, and J. Xiao, "Rethinking data augmentation for robust visual question answering," in *ECCV*, 2022, pp. 95–112.
- [132] Y. Liu, Y. Guo, J. Yin, X. Song, W. Liu, L. Nie, and M. Zhang, "Answer questions with right image regions: A visual attention regularization approach," *ACM TOMM*, pp. 1–18, 2022.
- [133] X. Han, S. Wang, C. Su, Q. Huang, and Q. Tian, "General greedy de-bias learning," *IEEE TPAMI*, pp. 1–17, 2023.

- [134] J. W. Cho, D.-j. Kim, H. Ryu, and I. S. Kweon, "Generative bias for visual question answering," in *CVPR*, 2023.
- [135] J. Liu, C. Fan, F. Zhou, and H. Xu, "Be flexible! learn to debias by sampling and prompting for robust visual question answering," *IPM*, vol. 60, p. 103296, 2023.
- [136] W. Wang, J. Gao, and C. Xu, "Weakly-supervised video object grounding via causal intervention," *IEEE TPAMI*, vol. 45, no. 3, pp. 3933–3948, 2023.
- [137] X. Wang, Y. Wu, A. Zhang, F. Feng, X. He, and T.-S. Chua, "Reinforced causal explainer for graph neural networks," *IEEE TPAMI*, vol. 45, no. 2, pp. 2297–2309, 2023.
- [138] L. Wang and K.-J. Yoon, "Knowledge distillation and student-teacher learning for visual intelligence: A review and new outlooks," *IEEE TPAMI*, vol. 44, no. 6, pp. 3048–3068, 2022.
- [139] H.-J. Ye, S. Lu, and D.-C. Zhan, "Generalized knowledge distillation via relationship matching," *IEEE TPAMI*, vol. 45, no. 2, pp. 1817–1834, 2023.
- [140] Y. Bengio, J. Louradour, R. Collobert, and J. Weston, "Curriculum learning," in *ICML*, 2009, pp. 41–48.
- [141] G. Gao, H. Huang, C. Fu, Z. Li, and R. He, "Information bottleneck disentangle for identity swapping," in *CVPR*, 2021, pp. 3404–3413.
- [142] T. Chen, S. Kornblith, M. Norouzi, and G. Hinton, "A simple framework for contrastive learning of visual representations," in *ICML*, 2020, pp. 1597–1607.
- [143] J. Park and J. Johnson, "Rgb no more: Minimally-decoded jpeg vision transformers," in *CVPR*, 2023, pp. 22 334–22 346.
- [144] R. R. Shetty, M. Fritz, and B. Schiele, "Adversarial scene editing: Automatic object removal from weak supervision," in *NeurIPS*, 2018, pp. 7717–7727.
- [145] C. Finn, P. Abbeel, and S. Levine, "Model-agnostic meta-learning for fast adaptation of deep networks," in *ICML*, 2017, pp. 1126–1135.
- [146] P.-S. Huang, C. Wang, R. Singh, W.-t. Yih, and X. He, "Natural language to structured query generation via meta-learning," in *NAACL*, 2018, pp. 732–738.
- [147] D. Teney and A. van den Hengel, "Visual question answering as a meta-learning task," in *ECCV*, 2018, pp. 219–235.
- [148] X. Wang and G.-J. Qi, "Contrastive learning with stronger augmentations," *IEEE TPAMI*, vol. 45, no. 5, pp. 5549–5560, 2023.
- [149] C.-Y. Chuang, J. Robinson, Y.-C. Lin, A. Torralba, and S. Jegelka, "Debiased contrastive learning," in *NeurIPS*, 2020, pp. 8765–8775.
- [150] P. Khosla, P. Teterwak, C. Wang, A. Sarna, Y. Tian, P. Isola, A. Maschinot, C. Liu, and D. Krishnan, "Supervised contrastive learning," in *NeurIPS*, vol. 33, 2020, pp. 18 661–18 673.
- [151] P. Liu, W. Yuan, J. Fu, Z. Jiang, H. Hayashi, and G. Neubig, "Pre-train, prompt, and predict: A systematic survey of prompting methods in natural language processing," *ACM Computing Surveys*, vol. 55, no. 9, pp. 1–35, 2023.
- [152] K. Zhou, J. Yang, C. C. Loy, and Z. Liu, "Conditional prompt learning for vision-language models," in *CVPR*, 2022, pp. 16 816–16 825.
- [153] P. Xu, X. Zhu, and D. A. Clifton, "Multimodal learning with transformers: A survey," *IEEE TPAMI*, 2023.
- [154] W. Kim, B. Son, and I. Kim, "Vilt: Vision-and-language transformer without convolution or region supervision," in *ICML*, 2021, pp. 5583–5594.
- [155] N. Yu, X. Hu, B. Song, J. Yang, and J. Zhang, "Topic-oriented image captioning based on order-embedding," *IEEE TIP*, vol. 28, no. 6, pp. 2743–2754, 2018.
- [156] S. Ye, J. Han, and N. Liu, "Attentive linear transformation for image captioning," *IEEE TIP*, vol. 27, no. 11, pp. 5514–5524, 2018.
- [157] M. Yang, J. Liu, Y. Shen, Z. Zhao, X. Chen, Q. Wu, and C. Li, "An ensemble of generation-and retrieval-based image captioning with dual generator generative adversarial network," *IEEE TIP*, vol. 29, pp. 9627–9640, 2020.
- [158] H. Song, L. Dong, W. Zhang, T. Liu, and F. Wei, "Clip models are few-shot learners: Empirical studies on vqa and visual entailment," in *ACL*, 2022, pp. 6088–6100.
- [159] B. Cao, J. Cao, J. Gui, J. Shen, B. Liu, L. He, Y. Y. Tang, and J. T.-Y. Kwok, "Alignve: Visual entailment recognition based on alignment relations," *IEEE TMM*, 2022.
- [160] J. Lu, D. Batra, D. Parikh, and S. Lee, "Vilbert: Pretraining task-agnostic visiolinguistic representations for vision-and-language tasks," in *NeurIPS*, 2019, pp. 13–23.
- [161] W. Su, X. Zhu, Y. Cao, B. Li, L. Lu, F. Wei, and J. Dai, "Vi-bert: Pre-training of generic visual-linguistic representations," in *ICLR*, 2020.
- [162] X. Li, X. Yin, C. Li, P. Zhang, X. Hu, L. Zhang, L. Wang, H. Hu, L. Dong, F. Wei *et al.*, "Oscar: Object-semantics aligned pre-training for vision-language tasks," in *ECCV*, 2020, pp. 121–137.
- [163] A. Radford, J. W. Kim, C. Hallacy, A. Ramesh, G. Goh, S. Agarwal, G. Sastry, A. Askell, P. Mishkin, J. Clark *et al.*, "Learning transferable visual models from natural language supervision," in *ICML*, 2021, pp. 8748–8763.
- [164] J. Li, R. Selvaraju, A. Gotmare, S. Joty, C. Xiong, and S. C. H. Hoi, "Align before fuse: Vision and language representation learning with momentum distillation," in *NeurIPS*, 2021, pp. 9694–9705.
- [165] H. Bao, W. Wang, L. Dong, Q. Liu, O. K. Mohammed, K. Aggarwal, S. Som, S. Piao, and F. Wei, "Vlmo: Unified vision-language pre-training with mixture-of-modality-experts," in *NeurIPS*, 2022, pp. 32 897–32 912.
- [166] Z. Wang, J. Yu, A. W. Yu, Z. Dai, Y. Tsvetkov, and Y. Cao, "Simvlm: Simple visual language model pretraining with weak supervision," in *ICLR*, 2022.
- [167] J. Yu, Z. Wang, V. Vasudevan, L. Yeung, M. Seyedhosseini, and Y. Wu, "Coca: Contrastive captioners are image-text foundation models," *TMLR*, vol. 2022, 2022.
- [168] J. Li, D. Li, C. Xiong, and S. Hoi, "Blip: Bootstrapping language-image pre-training for unified vision-language understanding and generation," in *ICML*, 2022, pp. 12 888–12 900.
- [169] W. Wang, H. Bao, L. Dong, J. Bjorck, Z. Peng, Q. Liu, K. Aggarwal, O. K. Mohammed, S. Singhal, S. Som *et al.*, "Image as a foreign language: Beit pretraining for vision and vision-language tasks," in *CVPR*, 2023, pp. 19 175–19 186.
- [170] X. Chen, X. Wang, S. Changpinyo, A. Piergiovanni, P. Padlewski, D. Salz, S. Goodman, A. Grycner, B. Mustafa, L. Beyer *et al.*, "Pali: A jointly-scaled multilingual language-image model," *arXiv preprint arXiv:2209.06794*, 2022.
- [171] J. Li, D. Li, S. Savarese, and S. Hoi, "Blip-2: Bootstrapping language-image pre-training with frozen image encoders and large language models," *arXiv preprint arXiv:2301.12597*, 2023.
- [172] A. Fang, G. Ilharco, M. Wortsman, Y. Wan, V. Shankar, A. Dave, and L. Schmidt, "Data determines distributional robustness in contrastive language image pre-training (clip)," in *ICML*, 2022, pp. 6216–6234.
- [173] M. Zhou, L. Yu, A. Singh, M. Wang, Z. Yu, and N. Zhang, "Un-supervised vision-and-language pre-training via retrieval-based multi-granular alignment," in *CVPR*, 2022, pp. 16 485–16 494.
- [174] S. Ren, K. He, R. Girshick, and J. Sun, "Faster r-cnn: Towards real-time object detection with region proposal networks," in *NeurIPS*, 2015, pp. 91–99.
- [175] J. Redmon, S. Divvala, R. Girshick, and A. Farhadi, "You only look once: Unified, real-time object detection," in *CVPR*, 2016, pp. 779–788.
- [176] L. Dong, N. Yang, W. Wang, F. Wei, X. Liu, Y. Wang, J. Gao, M. Zhou, and H.-W. Hon, "Unified language model pre-training for natural language understanding and generation," in *NeurIPS*, 2019, pp. 13 063–13 075.
- [177] H. W. Chung, T. Fevry, H. Tsai, M. Johnson, and S. Ruder, "Re-thinking embedding coupling in pre-trained language models," in *ICLR*, 2020.
- [178] B. Wang, X. Deng, and H. Sun, "Iteratively prompt pre-trained language models for chain of thought," in *EMNLP*, 2022, pp. 2714–2730.
- [179] A. Dosovitskiy, L. Beyer, A. Kolesnikov, D. Weissenborn, X. Zhai, T. Unterthiner, M. Dehghani, M. Minderer, G. Heigold, S. Gelly *et al.*, "An image is worth 16x16 words: Transformers for image recognition at scale," in *ICLR*, 2021.
- [180] H. Chen, Y. Wang, T. Guo, C. Xu, Y. Deng, Z. Liu, S. Ma, C. Xu, C. Xu, and W. Gao, "Pre-trained image processing transformer," in *CVPR*, 2021, pp. 12 299–12 310.
- [181] Z. Liu, J. Ning, Y. Cao, Y. Wei, Z. Zhang, S. Lin, and H. Hu, "Video swin transformer," in *CVPR*, 2022, pp. 3202–3211.
- [182] J. Duan, L. Chen, S. Tran, J. Yang, Y. Xu, B. Zeng, and T. Chilimbi, "Multi-modal alignment using representation codebook," in *CVPR*, 2022, pp. 15 651–15 660.
- [183] B. Mustafa, C. Riquelme, J. Puigcerver, R. Jenatton, and N. Houlsby, "Multimodal contrastive learning with limoe: the language-image mixture of experts," in *NeurIPS*, 2022.

- [184] Z. Wang, J. Yu, A. W. Yu, Z. Dai, Y. Tsvetkov, and Y. Cao, "Simvlm: Simple visual language model pretraining with weak supervision," in *ICLR*, 2022.
- [185] A. Li, A. Jabri, A. Joulin, and L. Van Der Maaten, "Learning visual n-grams from web data," in *CVPR*, 2017, pp. 4183–4192.
- [186] A. Kolesnikov, L. Beyer, X. Zhai, J. Puigcerver, J. Yung, S. Gelly, and N. Houlsby, "Large scale learning of general visual representations for transfer," *arXiv preprint arXiv:1912.11370*, 2019.
- [187] X. Zhai, J. Puigcerver, A. Kolesnikov, P. Ruysen, C. Riquelme, M. Lucic, J. Djolonga, A. S. Pinto, M. Neumann, A. Dosovitskiy *et al.*, "A large-scale study of representation learning with the visual task adaptation benchmark," *arXiv preprint arXiv:1910.04867*, 2019.
- [188] T. Brown, B. Mann, N. Ryder, M. Subbiah, J. D. Kaplan, P. Dhariwal, A. Neelakantan, P. Shyam, G. Sastry, A. Askell *et al.*, "Language models are few-shot learners," in *NeurIPS*, 2020, pp. 1877–1901.
- [189] N. C. Mithun, R. Panda, E. E. Papalexakis, and A. K. Roy-Chowdhury, "Webly supervised joint embedding for cross-modal image-text retrieval," in *ACM MM*, 2018, pp. 1856–1864.
- [190] X. He and Y. Peng, "Fine-grained image classification via combining vision and language," in *CVPR*, 2017, pp. 5994–6002.
- [191] T. Wang, L. Yuan, X. Zhang, and J. Feng, "Distilling object detectors with fine-grained feature imitation," in *CVPR*, 2019, pp. 4933–4942.
- [192] M. Zolfaghari, Y. Zhu, P. Gehler, and T. Brox, "Crossclr: Cross-modal contrastive learning for multi-modal video representations," in *ICCV*, 2021, pp. 1450–1459.
- [193] J. Wu, Y. Liang, H. Akbari, Z. Wang, C. Yu *et al.*, "Scaling multi-modal pre-training via cross-modality gradient harmonization," in *NeurIPS*, 2022, pp. 36161–36173.
- [194] H. Akbari, L. Yuan, R. Qian, W.-H. Chuang, S.-F. Chang, Y. Cui, and B. Gong, "Vatt: Transformers for multimodal self-supervised learning from raw video, audio and text," in *NeurIPS*, 2021, pp. 24206–24221.
- [195] K. He, H. Fan, Y. Wu, S. Xie, and R. Girshick, "Momentum contrast for unsupervised visual representation learning," in *CVPR*, 2020, pp. 9729–9738.
- [196] A. Agrawal, I. Kajić, E. Bugliarello, E. Davoodi, A. Gergely, P. Blunsom, and A. Nematzadeh, "Rethinking evaluation practices in visual question answering: A case study on out-of-distribution generalization," *arXiv preprint arXiv:2205.12191*, 2022.
- [197] S. Shen, L. H. Li, H. Tan, M. Bansal, A. Rohrbach, K.-W. Chang, Z. Yao, and K. Keutzer, "How much can CLIP benefit vision-and-language tasks?" in *ICLR*, 2022.
- [198] X. Chen, J. Djolonga, P. Padlewski, B. Mustafa, S. Changpinyo, J. Wu, C. R. Ruiz, S. Goodman, X. Wang, Y. Tay *et al.*, "PaLI-X: On Scaling up a Multilingual Vision and Language Model," *arXiv preprint arXiv:2305.18565*, 2023.
- [199] H. Bao, W. Wang, L. Dong, Q. Liu, O. K. Mohammed, K. Aggarwal, S. Som, S. Piao, and F. Wei, "Vlmo: Unified vision-language pre-training with mixture-of-modality-experts," in *NeurIPS*, 2022, pp. 32897–32912.
- [200] H. Bao, W. Wang, L. Dong, and F. Wei, "Vl-beit: Generative vision-language pretraining," *arXiv preprint arXiv:2206.01127*, 2022.
- [201] R. M. Monarch, *Human-in-the-Loop Machine Learning: Active learning and annotation for human-centered AI*. Simon and Schuster, 2021.
- [202] M. Malinowski, M. Rohrbach, and M. Fritz, "Ask your neurons: A deep learning approach to visual question answering," *IJCV*, vol. 125, pp. 110–135, 2017.
- [203] A. Wang, A. Liu, R. Zhang, A. Kleiman, L. Kim, D. Zhao, I. Shirai, A. Narayanan, and O. Russakovsky, "Revise: A tool for measuring and mitigating bias in visual datasets," *IJCV*, vol. 130, no. 7, pp. 1790–1810, 2022.
- [204] A. Mogadala, M. Kalimuthu, and D. Klakow, "Trends in integration of vision and language research: A survey of tasks, datasets, and methods," *JAIR*, vol. 71, pp. 1183–1317, 2021.



**Jie Ma** (Member, IEEE) is an Assistant Professor in the School of Cyber Science and Engineering (Faculty of Electronic and Information Engineering) at Xi'an Jiaotong University, Xi'an, Shaanxi 710049, P.R. China. He is also a member of the Ministry of Education's Key Lab for Intelligent Networks and Network Security. His research interests cover natural language processing and trustworthy multimodality learning, focusing particularly on knowledge graph learning, robust visual question answering, and question dialogue. He has contributed to several top journals and conferences, including IEEE TIP, TNNLS, IJCAI, and WSDM. Furthermore, he has served as a program committee member for numerous conferences such as ICLR and AAAI, and reviewed manuscripts for multiple journals such as IEEE TIP and TNNLS. For more information, please visit <https://dr-majie.github.io/>.



**Pinghui Wang** (Senior Member, IEEE) is currently a professor with the MOE Key Laboratory for Intelligent Networks and Network Security, Xi'an Jiaotong University, Xi'an, China, and also with the Shenzhen Research Institute, Xi'an Jiaotong University, Shenzhen, China. His research interests include internet traffic measurement and modeling, traffic classification, abnormal detection, and online social network measurement.



**Dechen Kong** received the BE degree in Electrical Engineering and Automation from Xi'an Jiaotong University, China, in 2022. He is currently working toward the ME degree in Electronic and Information Engineering in Xi'an Jiaotong University. His research interests include multimodal learning, natural language processing and computer vision.



**Zewei Wang** received the BE degree in automation from Xi'an Jiaotong University, China, in 2022. He is currently working toward the ME degree in control science and engineering with the School of Electronic and Information Engineering, Xi'an Jiaotong University. His research interests include multimodal learning, knowledge graph learning, and visual question answering.



**Jun Liu** (Senior Member, IEEE) received the B.S. in computer science and technology in 1995 and the Ph.D. degree in systems engineering in 2004, both from Xi'an Jiaotong University, China. He is currently a Professor with the Department of Computer Science, Xi'an Jiaotong University. He has authored more than ninety research papers in various journals and conference proceedings. He has won the best paper awards in IEEE ISSRE 2016 and IEEE ICBK 2016. His research interests include NLP and e-learning. Dr. Liu currently serves as an associate editor of IEEE TNNLS from 2020, and has served as a guest editor for many technical journals, such as Information Fusion, IEEE SYSTEMS JOURNAL. He also acted as a conference/workshop/track chair at numerous conferences.



**Hongbin Pei** is currently an Assistant Professor in the School of Cyber Science and Engineering at Xi'an Jiaotong University, China. He received his B.S., M.S., and Ph.D. degrees from Jilin University, China, in 2012, 2015, and 2021, respectively. His research interests include Deep Learning, Graph Data Mining, and Data-Driven Complex System Modeling, with Applications to Chemistry and Public Health.



**Junzhou Zhao** received BS and PhD degrees in control science and engineering from Xi'an Jiaotong University, in 2008 and 2015, respectively. He is currently an associate professor with the School of Cyber Science and Engineering, at Xi'an Jiaotong University. His research interests include graph data mining and streaming data processing.